CHAPTER 2
Chitosan-based Nanocomposites

SREEJARANI K. PILLAI*[a] AND SUPRAKAS S. RAY[a,b]

[a] DST/CSIR Nanotechnology Innovation Centre, National Centre for
Nano-Structured Materials, Council for Scientific and Industrial Research,
Pretoria 0001, Republic of South Africa; [b] Department of Chemical
Technology, University of Johannesburg, Doornforntein 2018, Johannesburg,
Republic of South Africa
*Email: skpillai@csir.co.za

2.1 Introduction

In the area of nanotechnology, polymer matrix-based nanocomposites have
generated a considerable amount of attention in the recent literature. This area
has emerged with the recognition that nano-sized reinforcement materials, due
to their high surface area, aspect ratio, and dispersion, could yield significant
property enhancement in polymeric systems when compared to large-scale
particulate reinforcement.[1,2] In the past half century, although synthetic pet-
roleum-based polymers have been widely used in composite preparation for a
variety of applications, they have become a major source of waste disposal
problems due to their poor biodegradability.[3] As a result of the increasing
awareness concerning human impact on the environment and constant
increases in fossil resources prices, the last decade has seen the development of
efficient solutions to produce new environmentally friendly materials. Parti-
cular attention has been paid to the replacement of conventional petroleum-
based plastics with materials based on biopolymers, such as biodegradable
polyesters,[4–7] proteins,[8–10] or polysaccharides.[11–14] Within this strategy, poly-
saccharides are vital candidates because of their renewable and recyclable
nature and their biodegradable character, together with the fact that they

represent the most abundant fraction of biomass. Chitosan is one of the most widely exploited polysaccharides in various applications owing to its properties that depend on environmental variables such as pH, ionic strength, and electric field.[15]

Nano-biocomposites, obtained by adding nanofillers to biopolymers like chitosan, result in very promising materials since they show improved properties with preservation of the material biodegradability without eco-toxicity. Such materials are mainly destined for biomedical applications and different short-term applications, *e.g.* packaging, agriculture, and hygiene devices. They thus represent a strong and emerging answer for improved and eco-friendly materials.

This chapter reviews the recent developments in the area of chitosan-based nanocomposites, with a special emphasis on clay-containing nanocomposites of chitosan. It describes various nano-sized reinforcements, preparation and characterization of the nanocomposites, their properties and applications.

2.2 Structure and Properties of Chitosan

Chitin, poly[β-(1→4)-*N*-acetyl-D-glucosamine], is a natural polysaccharide of major importance, first identified in 1684 (see Figure 2.1). This biopolymer is synthesized by an enormous number of living organisms, such as arthropods, fungi, and yeast, and from other biological sources; considering the amount of chitin produced annually in the world, it is the most abundant polymer after cellulose. The most important derivative of chitin is chitosan. Contrary to chitin, chitosan is not widespread in the nature. It is found in some mushrooms (zygote fungi) and in the termite queen's abdominal wall. It is industrially
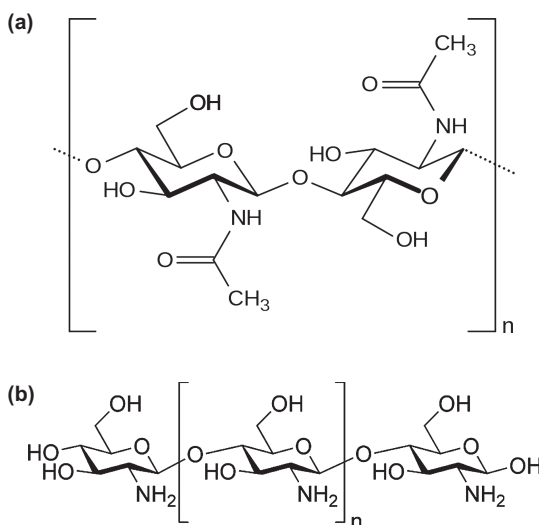

Figure 2.1   Chemical structures of (a) chitin and (b) chitosan.

obtained by (partial) deacetylation of chitin in the solid state under alkaline conditions (concentrated NaOH) or by enzymatic hydrolysis in the presence of chitin deacetylase. Its chemical structure, presented in Figure 2.1, is a random linear chain of *N*-acetyl-D-glucosamine units (acetylated unit) and D-glucosamine (deacetylated unit) joined by β-(1→4) linkages.[16] Conventionally, the distinction between chitin and chitosan is based on the degree of acetylation (DA), with chitin having DA values higher than 50% and chitosan having lower percentages. It follows that there is no unique polymer structure for chitosan, which gives this material properties which depend on its DA, as well as on its molecular weight.[15] According to the bioresource, industrial chitosan shows molecular weights ranging from 5 to 1000 kg mol^{-1}. In the solid state, chitosan is a semicrystalline polymer, and it can exist in different allomorphs depending on its DA, distribution of the acetyl groups along the carbohydrate chain, and the chitosan preparation procedure. Chitin and chitosan are biocompatible, biodegradable, and non-toxic polymers.[17]

2.2.1 Importance of Chitosan

Whereas chitin is insoluble in most solvents and difficult to process into useful materials, chitosan is readily soluble in dilute aqueous acidic solutions and is easily processed because of the amino groups present. Other advantages of this polymer include availability, low cost, high biocompatibility, biodegradability, antimicrobial property, ease of chemical modification, and excellent film-forming ability.[18] Chitosan also possesses properties including its high viscosity, charge distribution, and release mechanisms, making it particularly suitable as a carrier. Because of its unique properties, chitosan has attracted scientific and industrial interest in several fields, such as biotechnology, pharmaceutics, biomedicine, packaging, wastewater treatment, cosmetics, and food science.[19] Since chitosan is a haemostatic from which blood anticoagulants and anti-thrombogenics have been formed and can be easily processed into different forms such as gels, membranes, beads, micro-particles, nano-fibres, scaffolds, or sponges, it finds a variety of biomedical applications in tissue engineering, wound healing, drug delivery, *etc*.[20–24] Research into the chemical properties of chitosan has demonstrated its suitability for the preparation of enzymatic biosensors for the analysis of metallic elements, proteins, and lipids.[25,26] Chitosan has also been used as a coating for textile fibre protection and resistance and in paper and paperboard coating, *e.g.* for food packaging.[27]

In spite of the numerous advantages and unique properties of chitosan-based materials, they are not widely used to replace synthetic polymers because of their poor mechanical properties and moisture sensitivity. Moreover, its inherent properties, such as thermal stability, rigidity, and gas barrier properties, are often insufficient to meet the requirements of a number of applications. Consequently, to make them more suitable and competitive, both chemical and physical treatments of the materials are required.[28]

Many research studies have focused on improving the physical properties of chitosan materials by decreasing the hydrophilicity and improving the

mechanical properties. Hydrophobic materials, such as neutral lipids, fatty acids, or waxes, have been added to improve the moisture barrier properties of chitosan films.[29,30] One of the earliest methods to stabilize chitosan was to cross-link it with reagents like glutaraldehyde or to apply γ-irradiation.[31–33] The development of multiphase materials, *e.g.* blends or composites, where a reinforcing phase is added to chitosan, also represents a viable method of stabilization and improvement of properties.[34–36] Traditionally, micro-sized mineral fillers like silica, talc, and clay are added to reduce the cost and improve chitosan's performance in some way. However, the mechanical properties such as elongation at break and tensile strength of these composites decrease with the incorporation of these fillers.

2.2.2   Chitosan-based Nanocomposites

A new class of chitosan composite materials has emerged recently, based on the incorporation of reinforcing fillers with dimensions in the nanometric scale (nanofillers with at least one dimension within 100 nm).[11,37–39] Depending on the nature and surface functionality of the nanofillers, nanocomposites could exhibit modifications in their properties, such as improved mechanical and barrier properties, higher transparency,[40–43] *etc*. Such property enhancements rely on their nanoscale dispersion, even with a very low level of nanofiller incorporation (≤ 5 wt%), which results in a high aspect ratio and high surface area. The reinforcement efficiency of nanocomposites can match that of conventional composites with 40–50% of loading with classical fillers.[40] Nanocomposites with chitosan as the matrix and nano-sized reinforcements result in more stable and stronger materials. In these cases the percentage of reinforcing phase is normally low (5–10 wt%), to make the chitosan proportion relatively high. This results in products that closely resemble the matrix in terms of biocompatibility and bioactivity.

2.2.3   Importance of Chitosan-based Nanocomposites

Incorporation of nano-reinforcements into the chitosan matrix has been demonstrated as a powerful strategy to overcome the conventional drawbacks of the biopolymer. Nanocomposites of chitosan are potentially functional in a number of areas, including medicine, cosmetics, biotechnology, food industry, agriculture, environmental protection, paper industry, textiles, *etc*.

Chitosan can form nanocomposites with montmorillonite (MMT) clay, and there are several reports about the drug release behaviour from the chitosan/MMT nanocomposite films, scaffolds, and hydrogels.[44–48] Recent research studies have shown that chitosan/MMT composites represent an innovative and promising class of sorbent materials.[49,50] The use of chitosan-based nanocomposite coatings and films in the packaging industry has become a topic of great interest because of their potential for increasing the shelf-life of many food products.[51–53] The mechanical properties of composite scaffolds of

chitosan can be improved by the addition of nano-hydroxyapatite, bioactive glass ceramics which are widely used in tissue engineering.[54,55] A number of studies have reported recently on the use of chitosan nanocomposite scaffolds and membranes containing silver and gold nanoparticles to treat patients with deep burns, wounds, *etc.*, using their antimicrobial properties.[56,57] In the last few decades, the biosensor performance of chitosan materials has been significantly enhanced by the introduction of nanomaterials in the sensing layer, such as carbon nanotubes (CNTs),[58] nanowires,[59] and nanoparticles.[60] In addition to the enhancement in electrode and sensing abilities of chitosan materials, CNTs are reported to improve physical and mechanical properties, as well as the electric conductivities of the prepared chitosan/CNT nanocomposites.[61] The unique reinforcing behaviour of graphene sheets was also investigated in detail in chitosan biopolymers. Recent reports showed that the incorporation of 1 wt% graphene oxide improved the tensile strength and Young's modulus of graphene oxide/chitosan nanocomposites by 122% and 64%, respectively.[62,63] Currently, research on the composites of chitosan and metal oxide nanoparticles has focused on TiO_2 and ZnO, since they have excellent photocatalytic performance and are stable in acidic and alkaline solvents.[64,65] A combination of chitosan and magnetic nanoparticles such as Fe_3O_4[66] and $CoFe_2O_4$[67] are used in bio-applications, *e.g.* the immobilization of proteins, peptides, and enzymes, bio-affinity adsorbents, drug delivery, biosensors, and so on.[68–70] In summary, the emergence of nanotechnology is opening new horizons to chitosan-based materials, where nanoparticles have been utilized as stabilizing agents to improve their biocompatibility, film-forming ability, nontoxicity, and high mechanical strength. The nano-sized particles offer distinctively different physiochemical, magnetic, and optical properties compared to their bulk phase.

2.2.4 Types of Chitosan-based Nanocomposites

As mentioned above, chitosan nanocomposite properties depend on the type of nanofillers used, which in turn depend significantly on their shape, size, surface characteristics, and degree of dispersion in the chitosan matrix. To fulfil the definition of nanofiller, at least one of the particle dimensions has to be at nanometre scale ($\leq$100 nm). The different nanofillers can be classified depending on their aspect ratio and geometry, such as (i) platelet or layered particles (*e.g.*, clay, graphene), (ii) spherical (*e.g.*, silica or metal nanoparticles), or (iii) acicular or fibrous ones (*e.g.*, whiskers, carbon nanotubes).[39] The aspect ratio (ratio of particle length to thickness) is a key factor in defining the ability of a nanofiller to enhance the composite properties. For various nanofillers the aspect ratio increases in the following order: particles, platelets, and fibres, as demonstrated in Figure 2.2.

For example, nanoclay platelets have thickness in the range of 1 nm and a relatively high aspect ratio when compared to the spherical nanoparticles. Owing to the low aspect ratio, nanoparticles may not have an equally strong
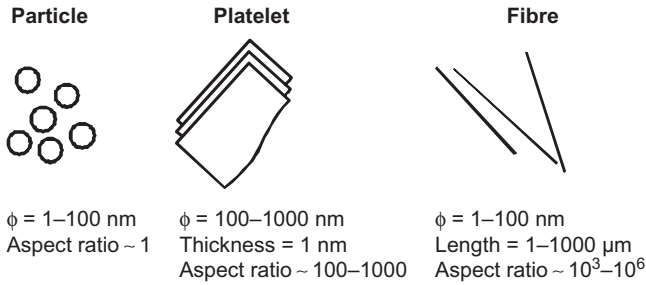
Particle   **Platelet**   **Fibre**

ϕ = 1–100 nm ϕ = 100–1000 nm ϕ = 1–100 nm
Aspect ratio ~ 1   Thickness = 1 nm   Length = 1–1000 µm
                       Aspect ratio ~ 100–1000   Aspect ratio ~ 10^3–10^6

Figure 2.2   Various nanofiller shapes and typical aspect ratios.

impact on mechanical property enhancement, but, on the other hand, they may provide surface softness, surface shine, *etc*. Nanofillers often possess high surface energies and are usually surface-modified to reduce the surface energy and prevent aggregation. Moreover, surface modification of the filler enhances the compatibility with the polymer matrix, which helps to achieve a good dispersion of the fillers. Table 2.1 gives a summary of different nanofillers used in chitosan matrices.

At present, the most intensive research is focused on layered silicates, due to their availability, versatility, and respectability towards the environment and health. Of the different groups of clay minerals such as kaolinite, smectite, illite, chlorite, and sepiolite, the most widely studied is the smectite group, because of its structural uniqueness (expansion and absorption properties). The most familiar species of the smectite group is MMT clay because of its large surface area, higher exchange capacity, abundance, and cost-effectiveness. Hence this chapter presents an overview of the recent progress in the field of chitosan nanocomposites based on MMT nanoclays.

2.3   Structure and Properties of Montmorillonite

MMT clay belongs to the same general family of 2:1 layered or phyllosilicates. MMT is the name given to the layered silicate found near Montmorillon in France, where it was first identified by Knight in 1696. Although MMT is found in vast deposits around the world, it is always found with impurities such as gravel, shale, limestone, quartz, and feldspar, among others. This mixture of materials is known as bentonite, and the MMT is separated from the raw ore primarily through aqueous separation processes. It consists of platelets with an inner octahedral layer sandwiched between two silicate tetrahedral layers,[91] as illustrated in Figure 2.3. The octahedral layer may be thought of as an aluminium oxide sheet where some of the aluminium atoms have been replaced with magnesium; the difference in valences of Al and Mg creates negative charges distributed within the plane of the platelets that are balanced by positive counter ions, typically alkali or alkaline earth cations, located between the platelets or in the galleries (see Figure 2.3). This type of layered silicate is

Table 2.1 Summary of various nanofillers used in chitosan matrices, the nanocomposite types, their preparation methods, and targeted applications.

Nanofiller type	Nano material used[a]	Nanocomposite type	Preparation method for chitosan nanocomposite	Application	Ref.
Particles	*Metal oxides* ZrO_2, Fe_3O_4, SiO_2, Cu_2O, TiO_2, ZnO, Al_2O_3	Thin films, hydrogels, powders	Electrophoretic deposition, ultrasonication, electro-chemical deposition, solution mixing, freeze drying	Biosensors for nucleic acid, drug delivery, enzyme immobilization, photocatalysis, water purification, tissue engineering, UV protection of fabrics, water treatment	71–77
	Metals Ag, Au, Pt, Pd, Co, Ni	Thin films, hydrogels	Solution mixing, spin coating, dip coating, co-precipitation, electrochemical deposition	Cell stimulation, antibacterial coatings, biosensors, catalysts, *etc.*	71–74
	Other Bioactive glass, CdS, quantum dots	Hydrogels, powders	Solution mixing, freeze drying	Thermo-responsive injectable scaffolds, tissue engineering, latent finger mark detection	75, 76
Fibres	SWCNTs, MWCNTs, Fe nanowires, ZnO nanowires, Au nanowires, nanorods, cellulose fibres	Composite fibres, powders, films	Solution spinning, freeze drying, solution mixing, sonication	pH, electrical actuators, bone tissue engineering, biological probes, electrochemical biosensors, paper coating	15, 77–83
Platelets	Layered silicates	Film, scaffolds, powders	Solution mixing, freeze drying, micro-emulsion process	Fuel cells, gas separation, drug delivery, water treatment, catalysis	45, 84–87
	Graphene, graphene oxide	Films, powders	Solution casting and mixing	Biosensing and electrochemical sensing	62, 88–90

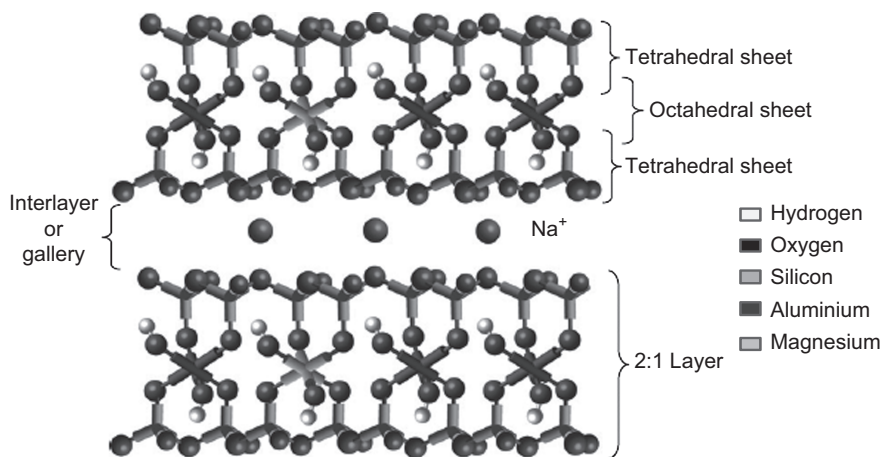[a]SWCNTs = single-walled carbon nanotubes; MWCNTs = multi-walled carbon nanotubes.

Figure 2.3 Structure of sodium montmorillonite.
(Reproduced with permission from Paul and Robeson.[1])

characterized by a moderate surface charge known as the cation exchange
capacity (CEC), which is generally expressed as mequiv per 100 g. This charge is
not locally constant, but varies from layer to layer, and must be considered as
an average value over the whole crystal.[1,92]

The chemical formula of MMT is $M_x(Al_{4-x}Mg_x)Si_8O_{20}(OH)_4$. MMT's CEC
(generally 90–110 mequiv per 100 g) and particle length (100–150 nm) depends
on the source. The specific surface area of MMT is equal to 750–800 $m^2\,g^{-1}$ and
the modulus of each MMT sheet is around 170 GPa. In its natural state, this
clay exists as stacks of many platelets. Hydration of the sodium ions causes
the galleries to expand and the clay to swell; indeed, these platelets can be
fully dispersed in water. The interlayer thickness of hydrated MMT is equal
to 1.45 nm, and the average density is $\rho = 2.385\,g\,mL^{-1}$. Drying MMT at 150 °C
reduces the gallery height to 0.28 nm, which corresponds to a water monolayer,
and hence the interlayer spacing decreases to 0.94 nm and the average density
increases to 3.138 $g\,mL^{-1}$.[40]

Pristine MMT usually contains hydrated Na^+ or K^+ ions.[93] Obviously, in
this pristine state, MMT particles are only miscible with hydrophilic polymers,
such as poly(ethylene oxide) (PEO), poly(vinyl alcohol) (PVA), *etc.*[94,95] To
render MMT particles miscible with chitosan polymer matrices, one must
convert the normally hydrophilic silicate surface to an organophilic one,
making the intercalation of chitosan chains possible. A chemical modification
of the clay surface, with the aim to match the polymer polarity, is often
achieved.[39,92] Cationic exchange is the most common technique, but other
original techniques such as organosilane grafting,[96,97] the use of ionomers,[98,99]
or block copolymer adsorption[100] are also used. Generally, cation exchange
consists of the substitution of inorganic cations by organic ones. These
are often primary, secondary, tertiary, or quaternary alkylammonium or
alkylphosphonium cations. Alkylammonium or alkylphosphonium cations

Table 2.2 Commercially available MMT clays and their characteristics.

Commercial Supplier/clays	Designation	Modifier	Modifier concentration (mequiv per 100 g)	Weight loss on ignition, Δw (%)	d-spacing (Å)
Southern Clay Products (USA)					
Cloisite Na	CNa	None	–	7	11.7
Cloisite 15A	C15A	$^+NMe_2(tallow)_2$	125	43	31.5
Cloisite 20A	C20A	$^+NMe_2(tallow)_2$	95	38	24.2
Cloisite 25A	C25A	$^+NMe_2(C_8)(tallow)$	95	34	16.6
Cloisite 93A	C93A	$^+NHMe(tallow)_2$	90	37.5	23.6
Cloisite 30B	C30B	$^+NMe(EtOH)_2(tallow)$	90	30	16.5
Süd-Chemie (Germany)					
Nanofil 804	N804	$^+NMe(EtOH)_2(tallow)$	105	21	16
Laviosa Chimica Mineraria (Italy)					
Dellite LVF	LVF	None	–	4–6	9.8
Dellite 43B	D43B	$^+NMe_2(CH_2Ph)(tallow)$	95	32–35	16.6

(known as "surfactants") in the organosilicates lower the surface energy of the inorganic host and improve the wetting characteristics of the polymer matrix, resulting in a larger interlayer spacing. Additionally, the surfactants can provide functional groups that can react with the polymer matrix, or in some cases initiate the polymerization of monomers to improve the adhesion between the inorganic salt and the polymer matrix.[101] Different types of organically modified MMTs, which differ in the nature of their counter cation and CEC, are commercially available, for example Cloisite 15A (C15A), Cloisite 20A (C20A), Cloisite 30B (C30B), Nanofil, *etc*. Table 2.2 presents the characteristics of some of the commercially available organically modified MMTs.

2.4 Nanocomposites: Preparation, Structure, and Characterization

Intercalation of polymers with the layered silicate has proven to be a successful approach to synthesize nanocomposites. Nanocomposites can, in principle, be formed from clays (pristine and organically modified) by three main methods:[40] (i) *in situ* polymerization, (ii) solvent intercalation, and (iii) the melt intercalation process. The solvent intercalation route consists of swelling the layered silicates in a polymer solvent to promote diffusion of the macromolecules in the clay interlayer spacing. The *in situ* intercalation method causes the layered silicates to swell in the monomer or monomer solution before polymerization. The melt intercalation process is based on polymer processing in the molten

state, such as extrusion. Obviously, the last method is highly preferred in the
context of sustainable and eco-friendly development since it avoids the use of
organic solvents.[102]

For most purposes, complete exfoliation of the clay platelets, *i.e.* separation
of the platelets from one another and dispersal individually in the polymer
matrix, is the desired goal of the formation process. However, this ideal mor-
phology is frequently not achieved and varying degrees of dispersion are more
common. The literature often refers to three main types of morphology:
immiscible (conventional or microcomposite), intercalated, and exfoliated. For
microcomposites, the polymer chains have not penetrated into the interlayer
spacing and the clay particles are aggregated. In the intercalated structures, the
polymer chains have diffused between the platelets, leading to an increase in
intergallery spacing. In the exfoliated state, the clay layers are individually
delaminated and homogeneously dispersed into the polymer matrix. Inter-
mediate dispersion states are often observed, such as intercalated exfoliated
structures. This classification does not take into account the dispersion multi-
scale structure, such as the percolation phenomenon, preferential orientation of
the clay layers, *etc.*[39,40,103]
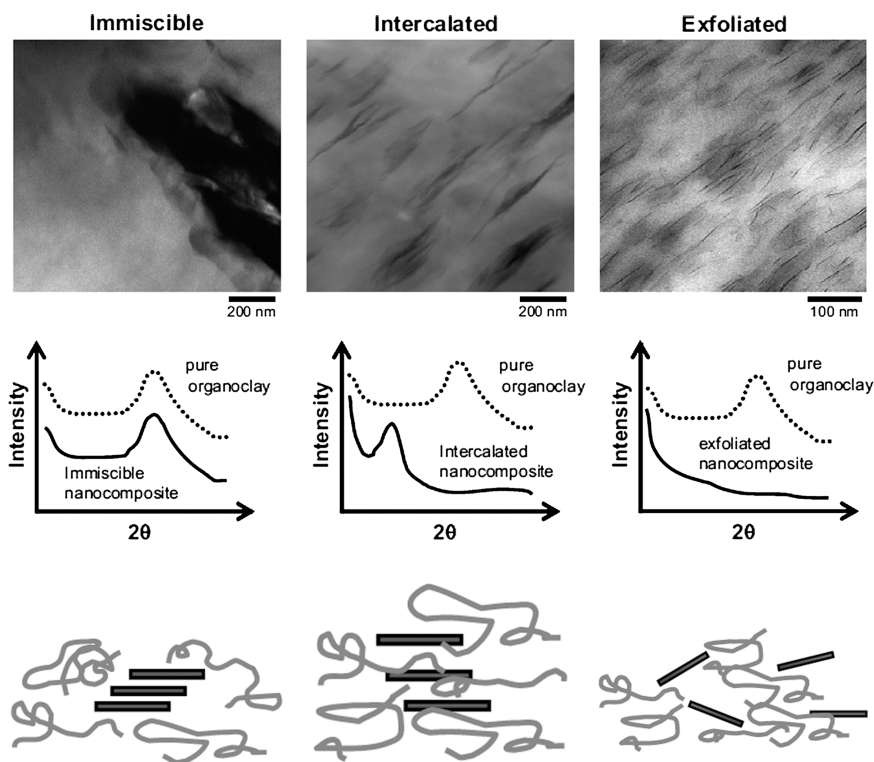

Figure 2.4   Illustration of different morphologies of polymer/MMT nanocomposites.
(Reproduced with permission from Paul and Robeson.[1])

The degree of intercalation and exfoliation of layered silicates in polymer nanocomposites can be quantified using X-ray diffraction (XRD) and transmission electron microscopy (TEM). For microcomposites, the wide-angle X-ray scan of the polymer composite is expected to look essentially the same as that obtained for the organoclay powder; there is no change of the X-ray *d*-spacing. The intercalated layered silicate has a defined interlayer spacing basal reflection corresponding to an increase in the gallery spacing calculated from XRD peak positions. For completely exfoliated organoclay, no wide-angle X-ray diffraction peak is expected for the nanocomposite since there is no regular spacing of the platelets and the distances between platelets would, in any case, be larger than what wide-angle X-ray scattering can detect.[104–106] TEM is a complementary technique to XRD wherein an image of the dispersion of the silicate within a polymer matrix can be quantified and analyzed. These are illustrated schematically in Figure 2.4, along with example TEM images and the expected XRD spectra.

2.5 Chitosan/MMT Nanocomposites

Chitin with a deacetylation degree of 75% or above is generally known as chitosan, which can be considered as a copolymer composed of glucosamine and *N*-acetylglucosamine units; it dissolves readily in dilute organic acids, providing a clear, homogeneous, and viscous solution.[107] Thus, the chemically active groups in the chitosan structure are the free amine groups, located in the C-2 position of the glucose residue in the polysaccharide chain, and the hydroxyl groups, with both being susceptible to modification. As a primary aliphatic polyamine, chitosan is involved in all of the reactions typical of amines. Most of the applications of chitosan are based on the polyelectrolytic nature and chelating ability of the amine group of the macromolecules, and such properties are mainly governed by the acidity of the $-NH_3^+$ group.[108] The weak-base anion-exchange ability of pure chitosan has been applied in the development of chitosan-based films for chemical and biosensing applications.[25,109]

However, these materials have poor performance because of the lack of long-term stability due to alteration of the characteristics of chitosan with time. Recent research has indicated that incorporation of pristine or organically modified MMT shows much promise for chitosan-based polymer nanocomposites in terms of improvements in their mechanical properties and stability over those of the unfilled formulations.[110] Because of the polycationic nature of chitosan in acidic media, this biopolymer appears as an excellent candidate for intercalation in MMT silicate layers by means of a cationic exchange process.

2.5.1 Preparation Methods and Characterization

In the case of natural polymers, the choice of a suitable method for the preparation of nanocomposites is limited by the processing possibilities of the natural materials. Since nature itself produces the possible matrix polymers,

only blending/compounding with suitable inorganic particles, either in the melt
or in solution, is an accessible manufacturing possibility.[111] Recently, a new
alternative method for the preparation of nanocomposites, which involves
solid-state mixing at room temperature (ball milling),[112] was proposed.

Darder *et al.*[113,114] prepared chitosan/MMT nanocomposite by a conven-
tional method whereby the chitosan solution in acetic acid with a pH of 4.9 was
added to 2 wt% Cloisite Na (CNa) suspension and magnetically stirred for
2 days. The final mixture was filtered, washed, and air dried at 50 °C to obtain
the composite powder. Nanocomposites with different chitosan/CNa ratios
(0.25:1, 0.5:1, 1:1, 2:1, 5:1, and 10:1) were prepared and compared. The XRD
spectra for the 1:1 chitosan/MMT ratio showed an increase of the basal
spacing, which is an indication of intercalation of chitosan with the silicate
layers. The scanning transmission electron microscopy (STEM) images
(Figure 2.5) of composites with a lower chitosan content showed the char-
acteristic platelets of the montmorillonite tactoids, whereas the composites with
chitosan/CNa ratios of 5:1 consisted essentially of well-intercalated phases.

Yu *et al.*[115] prepared a new nanocomposite consisting of poly(butyl acrylate),
chitosan, and methyltrioctadecylammonium bromide-modified MMT by γ-ray
irradiation polymerization in aqueous acetic acid solution. XRD results
showed that the layers of MMT are intercalated and orderly dispersed in this
nanocomposite. Lin *et al.*[116] reported on a novel method for the preparation of
chitosan/MMT nanocomposite films using a solvent casting method. The
MMT was incorporated with potassium persulfate (KPS) in aqueous solution
through cationic exchange first and then mixed with the acidified aqueous
solution of chitosan, and the composites were cast to form films. The shifting of
the characteristic MMT peak in the XRD patterns of the composite films
suggested that the MMT had been almost fully exfoliated, which was supported
by the TEM results. The higher the quantity of the KPS incorporated into the
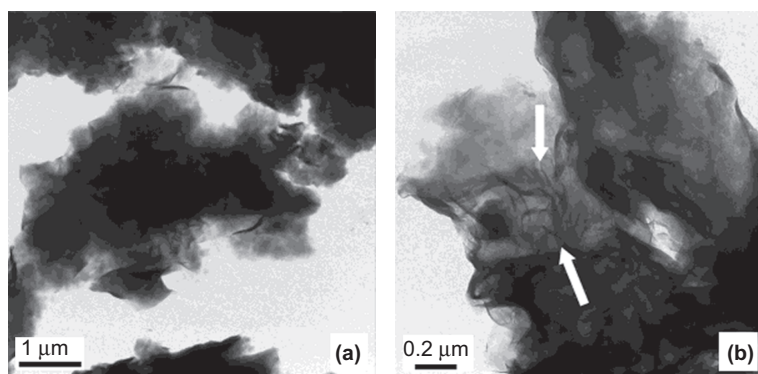MMT, the more the MMT exfoliated. As the KPS-incorporated MMT was

Figure 2.5   STEM images of nanocomposites prepared from chitosan/CNa ratios of
(a) 1:1 and (b) 5:1.
(Reproduced with permission from Darder *et al.*[113])

dispersed in the acidified aqueous solution of chitosan, the KPS instantly
reacted with the chitosan, resulting in cleavage of the polymer chains which
triggered the exfoliation of MMT. Wang *et al.*[117] used a similar method
for the preparation of chitosan/MMT composites with 2.5, 5, and 10 wt%
MMT content. The XRD patterns and TEM images clearly illustrated that the
MMT keeps intercalated and exfoliated structures at the lower MMT content
of 2.5 wt%, while on increasing the MMT content the MMT layers assemble
to form intercalated and flocculated structures due to a hydroxylated edge
interaction of the silicate layers.

Xu *et al.*[46] prepared chitosan-based nanocomposite films with CNa and
C30B using a solvent casting method. Structural characterization using XRD
and TEM indicated that the silicate layers were exfoliated in the chitosan
matrix with small amounts of Na-MMT, and that the intercalation with some
exfoliation occurred with up to 5 wt% Na-MMT. However, microcomposites
(tactoids) formed when C30B was added to the chitosan matrix. For C30B the
clay became organic and its hydrophobicity increased. Hence it is very difficult
to disperse C30B in the chitosan aqueous solution and to form an inter-
molecular reaction between clay and chitosan in spite of the presence of
hydroxyl groups in the gallery of the C30B.

Rhim *et al.*[118] developed an antimicrobial chitosan film containing CNa and
C30B and found that the film incorporated with C30B had significantly higher
antimicrobial activity than the CNa-containing system. This may be ascribed to
the antimicrobial activity of the quaternary ammonium group in the silicate
layer of the C30B incorporated film.

On the other hand, Han *et al.*[119] recently reported enhanced antimicrobial
activity of chitosan/Na-MMT composite films. Formation of exfoliated
nanocomposites of chitosan upon incorporation of small amounts of C10A was
reported by Oguzlu and Tihminlioglu.[120] For such nanocomposites the inter-
calated structure becomes dominant when the clay content is higher than 2 wt%.

In another recent study, Sahoo *et al.*[121] prepared a blend of chitosan, poly-
caprolactone (80:20 ratio), and C30B by solution mixing. The results indicated
that interaction of C30B occurs together with exfoliation and the extent of
interaction increases with an increase in clay concentration from 1 to 5 wt%.
According to the authors, during the mixing process the external platelets of
C30B are subjected to dynamic high shear forces that ultimately cause their
delamination from the stack of layers building the C30B particles, and then an
onion-like delamination process continues to disperse the platelets of silicate
into the polymer matrix. Blends of chitosan, poly(lactic acid), and C30B were
prepared by Nanda *et al.*[122] by a similar procedure.

Wang *et al.*[123] used two kinds of chitosan derivatives, namely *N,O*-carboxy-
methyl chitosan and *N,N,N*-trimethyl chitosan chloride, to prepare nano-
composite films with MMT clay by a solution casting method. The XRD and
TEM results indicated that introduction of the carboxymethyl functional
groups into chitosan chains causes a strong reaction with the silicate hydroxy-
lated edge groups through hydrogen bonding, leading to the assembly of
MMT in the polymer matrix to form a strong flocculated structure. On the

other hand, a quaternized amino group in chitosan improved its aqueous
solubility, made the polymer cationic, and exfoliation of MMT layers is
therefore favoured. Intercalation of quaternized chitosan chains into the Na-
MMT silicate layers was also reported by Choudhari and Kariduraganavar.[124]

Depan and co-workers[48,84] synthesized nanocomposites of lactic acid-grafted
chitosan and layered silicates by dissolving chitosan and dispersing CNa in an
aqueous solution of L-lactic acid, with subsequent heating and film casting. A
decrease in the 2θ value and an increase in d-spacing in the XRD spectra of the
samples confirmed the intercalation of biopolymer in the clay galleries. This
result was supported by TEM and EDX analyses.

Zhang *et al.*[125] prepared a novel chitosan-*g*-poly(acrylic acid)/MMT super-
absorbent nanocomposite by *in situ* intercalative polymerization among
chitosan, acrylic acid, and MMT in aqueous solution, using N,N'- methyle-
nebisacrylamide as a cross-linker and ammonium persulfate as an initiator.
XRD, IR, and TEM analyses showed that *in situ* graft polymerization resulted
in exfoliation of MMT and the chitosan chains could intercalate into layers of
MMT to form nanocomposites. From the SEM images shown in Figure 2.6,
the surface of the MMT-containing nanocomposite seemed to be more porous
compared to that of its counterpart without the clay filler, which is ideal for
water penetration. The authors claim that this one-step method is more con-
venient and the corresponding nanocomposites have higher swelling ability and
pH responsivity compared to the two-step method.

Wang and co-workers[126,127] prepared and compared the properties of chit-
osan/MMT and chitosan/cetyltrimethylammonium bromide (CTAB)-modified
MMT nanocomposites. The TEM and XRD results showed that a better dis-
persion of clay nanoplatelets was achieved by the modification of the clay with
CTAB, which indicated the formation of an exfoliated nanostructure in the
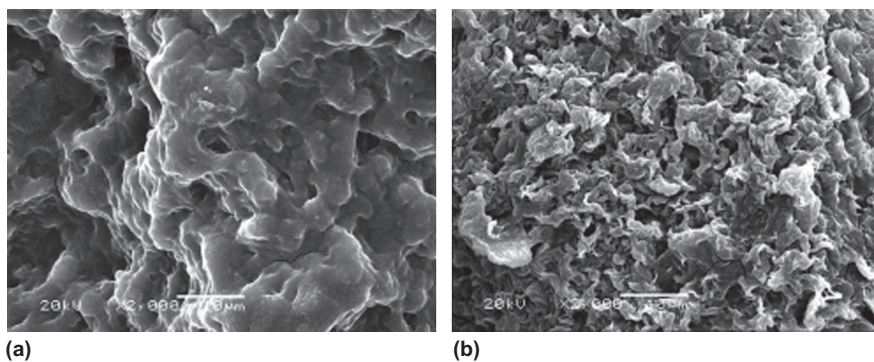nanocomposite.

(a)   (b)

Figure 2.6   SEM micrographs of (a) chitosan-*g*-poly(acrylic acid) and (b) chitosan-*g*-
poly(acrylic acid)/MMT nanocomposite prepared using the one-step
method. Weight ratio of acrylic acid to chitosan is 7.2; MMT content in
the feed is 10 wt %.
(Reproduced with permission from Zhang *et al.*[125])

A novel method of synthesis of chitosan/MMT nanocomposites in the presence of hydroxyaluminium cations was reported by Tan *et al.*[128] In this procedure, the chitosan solution, the MMT suspension, and the pillaring solution of hydroxyaluminium oligomeric cations {aluminium Keggin ions $[Al_{13}O_4(OH)_{24}(H_2O)_{12}]^{7+}$} with a ratio of 10 mmol Al per g of MMT were solution mixed and stirred for 2 days at 60 °C. The mixture was finally filtered, washed, and air dried. The intercalation of the biopolymer and hydroxyaluminium cation in the clay interlayer was confirmed by the decrease of 2θ values from 4.7 to 4.62–4.38, corresponding to a d_{001} value of 1.91–2.02 nm (Figure 2.7). In this study, the nanocomposites with bilayer chitosan were obtained at a chitosan/clay ratio of about 3:1 (against a ratio of 5:1 reported by Darder *et al.*[113]), which indicates that the presence of the hydroxyaluminium
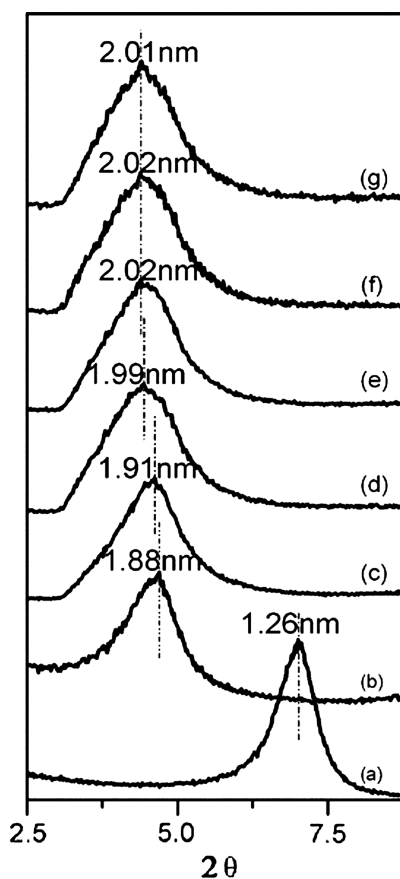

Figure 2.7 XRD patterns of (a) Na-MMT, (b) Al-pillared MMT, and nanocomposites prepared from chitosan-CEC at MMT ratios of (c) 1:1, (d) 2:1, (e) 3:1, (f) 4:1, and (g) 6:1.
(Reproduced with permission from Tan *et al.*[128])

cations can accelerate the intercalation procedure and decrease the dosage of   1
chitosan.

Zhang and Wang[129] developed chitosan/Na-MMT/multi-walled carbon
nanotube (MWCNT) nanocomposite films by a simple solution–evaporation
method. In a typical procedure, the required amount of MMT and MWCNTs   5
were suspended in distilled water and sonicated. An acetic acid solution of
chitosan was then added to the mixture and mechanically stirred for 20 min.
This solution was then used to form uniform nanocomposite films by solvent
casting. The XRD results indicated the exfoliation of MMT layers in the
polymer matrix. The introduction of MWCNTs increased the mechanical   10
properties of the nanocomposite without affecting the interfacial interaction of
the chitosan and MMT layers.

Yao and co-workers[130] introduced a novel approach to fabricate artificial
nacre-like chitosan/MMT bionanocomposite films by self-assembly of chit-
osan/MMT hybrid building blocks, as illustrated in Figure 2.8. The fabrication   15
process was simple, fast, time-saving, and could be easily scaled up. In this
method, milky white colloidal chitosan/MMT hybrid building blocks were first
prepared by mixing an aqueous suspension of exfoliated MMT nanosheets and
an aqueous solution of chitosan and stirring to guarantee full adsorption of
chitosan on the MMT nanosheets. The chitosan/MMT hybrid building blocks   20
were then aligned into the nacre-like structured composite by self-assembly
induced by vacuum filtration or water evaporation.

Lavorgna et al.[131] studied the effect of the presence of glycerol as a plasticizer
in chitosan/MMT films prepared by the solution casting method. The XRD
results suggested that in films without glycerol the Na-MMT stacks lay with   25
their platelets parallel to the casting surface, forming a flocculated structure
which is attributed to the hydrogen-bonding interactions between the hydro-
xylated edge–edge of the silicate layers and the amino or hydroxyl functional
groups of chitosan. The addition of the glycerol plasticizer, on the other hand,
reduces the extent of hydrogen-bonding interactions between chitosan and the   30
MMT edges by favouring preferential interactions between glycerol molecules
and edge-MMT. This hinders the flocculation process and facilitates the
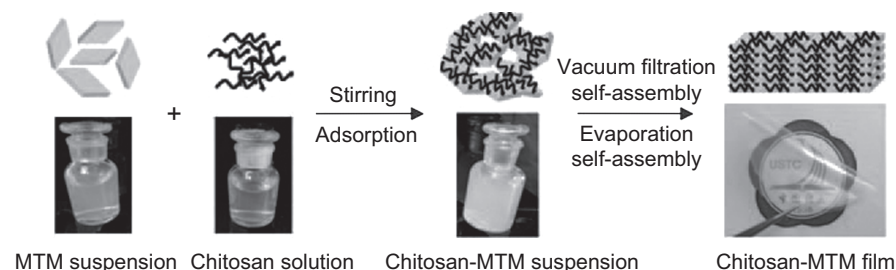intercalation, leaving the MMT stacks randomly oriented in the film.

MTM suspension   Chitosan solution   Chitosan-MTM suspension   Chitosan-MTM film

Figure 2.8   Fabrication of artificial nacre-like chitosan/MMT bionanocomposite
films.
(Reproduced with permission from Yao et al.[130])

Recently, Shameli *et al.*[132,133] prepared Ag/MMT/chitosan composites using a green UV irradiation method. In a typical procedure, 500 mL of AgNO₃ (0.02 M) was added to the chitosan solution in acetic acid under constant stirring. This solution was then added to the clay suspension and stirred vigorously at room temperature. The mixture was then irradiated with UV light for different time intervals at $\lambda = 365$ nm while it was stirred at a speed of 195 rpm. The TEM results showed successful incorporation of Ag nanoparticles in the chitosan/MMT matrix. It was found that the increase in UV irradiation time caused a decrease in particle size and size distribution. The XRD confirmed a face-centred cubic lattice for the Ag crystals and intercalation of chitosan in the MMT structure.

In conventional processing techniques, such as extrusion, compression, and injection moulding, the specific mechanical energy, shear impact, pressure, plasticizer, time, and temperature are important parameters to determine the clay dispersion and chemical cross-linking which ultimately define the composite properties. In wet processing, the extent of the interaction of clay with the chitosan depends mainly on the surface modification of the clay and functional groups on the polymer and the film-forming conditions such as the drying temperature and drying rate, the moisture content, the solvent type, the plasticizer concentration, and the pH.

The organic modifier plays an important role in producing the nanocomposite. It may either enhance the interaction between the clay and the polymer, making it more suitably mixed, or it may favour the intercalation of the polymer chain by dictating the gallery spacing. Most of the studies on the preparation of chitosan/MMT clays given in this section indicate that, irrespective of whether the clays are organically modified or not, a lower concentration of MMT clay (mostly 1–5 wt%) favours the formation of exfoliated or intercalated structures, whereas at a higher clay content the clay layers interact to form flocculated structures.

Full exfoliation (individual platelet dispersion) of nanoclay in a chitosan matrix by using conventional preparation techniques is still very difficult owing to the large lateral dimensions of the layers and a strong inclination of clay platelets to aggregate. However, the degree of exfoliation can be improved to some extent by optimizing the processing conditions such as shear forces or mixing rates when using extruders, mixers, ultrasonicators, ball milling, *etc*.

2.5.2 Properties

Bionanocomposites consisting of chitosan and MMT (organically modified or not) frequently exhibit moderate enhancement in mechanical and various other properties when compared to neat chitosan. Improvements generally include a higher modulus, both in the solid and melt states, increased strength and thermal stability, reduced gas permeability, and better biodegradability. The main reason for these improved properties in nanocomposites is the stronger interfacial interaction between the matrix and layered silicate with nanoscale dimensions, against the conventional microfiller-reinforced systems.

2.5.2.1   Mechanical Properties

A general reason for adding fillers to polymers is to increase the modulus or stiffness *via* reinforcement mechanisms described by theories for composites.[134,135] Properly dispersed and aligned clay platelets have proven to be very effective for increasing the stiffness of polymer matrices. The level of adhesion of the clay platelets to the polymer matrix is also crucial in deciding the mechanical properties of the resultant nanocomposites. Dynamic mechanical analysis (DMA) is one of the methods by which we can measure viscoelastic properties of a material when subjected to oscillatory deformation through controlled stress or strain. Under the applied stress, most polymeric materials show a combination of elastic and viscous types of behaviour, *i.e.* they react elastically, flow to some extent at the same time, and are termed "viscoelastic". The stress and strain curves will be therefore out of phase. DMA measures the amplitudes of the stress and strain as well as the phase angle between them. This is used to resolve the modulus into an in-phase component, *i.e.* the storage modulus (G' or E'), and an out-of-phase component, *i.e.* the loss modulus (G'' or E''). The ratio of the loss to the storage moduli (G''/G') is tan delta (tan δ) and is often called the damping factor. It is a measure of the energy dissipation of a material, which is useful in measuring the glass transition temperature (T_g). Another procedure to understand the mechanical properties of a polymer nanocomposite is tensile testing. It predicts the behaviour of the material under different types of forces. Tensile tests produce a stress–strain diagram, which is used to determine the tensile modulus. Properties that are directly measured *via* a tensile test are ultimate tensile strength and maximum elongation (elongation at break). From these measurements, properties like Young's modulus and yield strength can also be determined.

Nanoindentation is another means of testing the mechanical properties of small volumes of material where small loads and tip sizes are used to measure the load-displacement properties and extract parameters like Young's modulus.

Xu *et al.*[46] studied the tensile properties of chitosan nanocomposite films containing CNa and C30B, and the results are summarized in Table 2.3. With the introduction of 1 and 3 wt% of CNa, the tensile strength of the composite films increased by 35 and 62%, which was suggested to be due to the exfoliated

Table 2.3   Mechanical properties of chitosan/nanoclay composites.

Materials	Tensile strength (MPa)	Elongation at break (%)
Chitosan	40.62 ± 0.84	13.14 ± 3.85
1% CNa	54.98 ± 4.83	8.72 ± 0.97
3% CNa	65.67 ± 2.20	10.81 ± 0.52
5% CNa	44.51 ± 3.91	8.98 ± 1.21
1% C30B	45.01 ± 0.16	14.40 ± 1.47
3% C30B	47.97 ± 4.91	5.71 ± 1.72
5% C30B	47.29 ± 3.10	4.42 ± 0.19

state and the uniform dispersion of MMT in the chitosan matrix. Aggregation of MMT nanoparticles with high surface energy resulted in a decrease of tensile strength at higher clay content. When C30B was added to the chitosan matrix, the tensile strength did not increase significantly, although it improved the load bearing capacity of the composites initially. This was attributed to the formation of microcomposites.

The effect of tricetadecylmethylammonium bromide (TRIAB)-modified MMT on the mechanical properties of hybrid composites of poly(butyl acrylate) and chitosan has been reported by Yu *et al.*[136] The nanocomposites exhibited an enhancement of the E' and tensile properties at relatively small amounts of TRIAB-modified MMT (≤ 3 wt%) loadings, whereas higher TRIAB-modified MMT loadings decreased the mechanical properties due to cluster formation. On the other hand, the T_g of the nanocomposite increased with the introduction of TRIAB-modified MMT. This is due to inhibition of the rearrangement of the bond structure of chitosan.

Lin *et al.*[137] investigated the tensile properties of chitosan/KPS-MMT nanocomposites with MMT incorporating various cation exchange capacities (CEC) of KPS. It was found that when 0.5 CEC KPS was used to incorporate with the MMT, the resulting nanocomposite had higher tensile strength but lower Young's modulus than the pristine chitosan. With increasing the amount of KPS incorporated in the MMT, more MMT exfoliated along with the degradation of chitosan so that the Young's modulus increased but the tensile strength decreased. Nevertheless, both of them were still much greater than those of the chitosan-containing KPS only.

The synergistic effect of MWCNTs and Na-MMT on the mechanical properties of chitosan was reported by Zhang and Wang.[129] The results given in Figure 2.9 indicate that MMT and MWCNTs simultaneously introduced into chitosan film can greatly improve the mechanical properties. The Young's modulus of the chitosan film is increased about 50% as 1.0 wt% MMT and 1.0 wt% MWCNTs are introduced. A very similar trend was observed in the case of tensile strength after the introduction of MWCNTs. Although the elongation at break decreased gradually with increasing MWCNT content, the MMT could compensate for the negative effect of the MWCNTs. The highest elongation at break is obtained when the contents of MMT and MWCNTs are 0.5 and 0.5 wt%, respectively. The $-NH_3^+$ groups on the chains of chitosan adsorbed on the surface of MWCNTs could interact with the negatively charged MMT sheets and form a third MMT$\cdots$chitosan$\cdots$MWCNTs subassembly, which may be responsible for the synergistic effect of MMT and MWCNTs on the mechanical properties of the neat chitosan film.

Yao *et al.*[130] compared the tensile properties of hybrid nanocomposites of chitosan and MMT prepared by three different techniques, namely conventional, evaporation, and self-assembly by vacuum filtration. The mechanical performance of the well-aligned artificial nacre-like film is better than that of the film made by conventionally simply mixing the constituents. The Young's modulus and ultimate tensile strength of the well-aligned artificial nacre-like films are respectively 3–5-fold and 2–3-fold higher than that of conventional
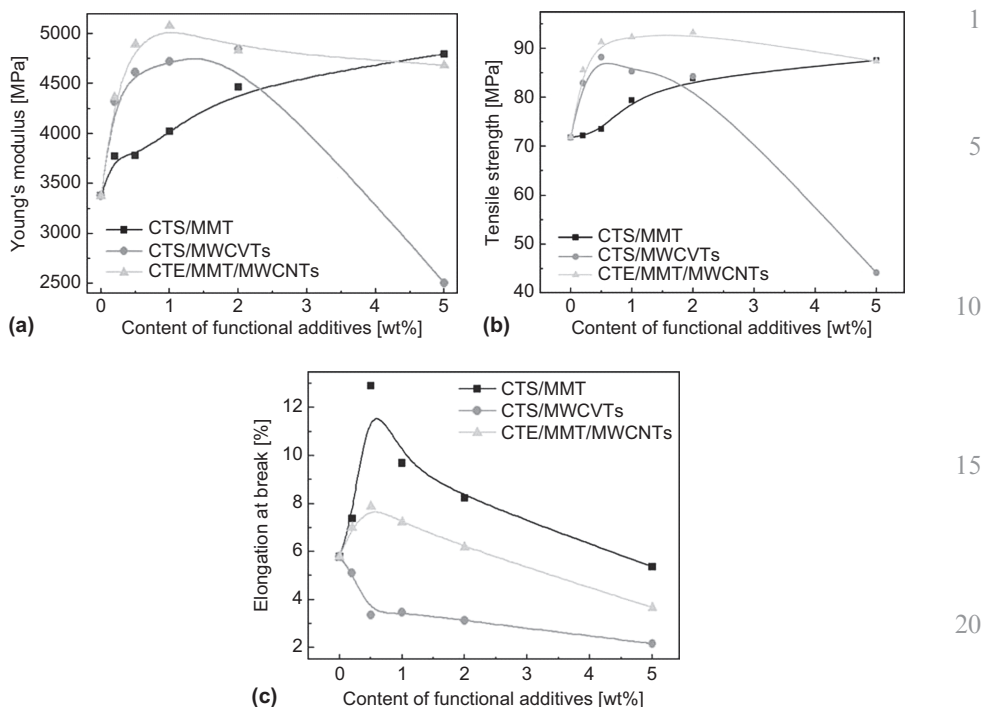
(a)

(b)

(c)

Figure 2.9 Variation of (a) Young's modulus, (b) tensile strength, and (c) elongation at break for chitosan/MMT, chitosan/MWCNTs, and chitosan/MMT/MWCNTs nanocomposite films with different additive contents. (Reproduced with permission from Zhang and Wang.[129])

film. The electrostatic attraction between the OH and NH_3^+ groups of chitosan and the MMT surface could contribute to the improvement in the mechanical properties of the nanocomposite.

An increase of approximately 80% in tensile strength and 50% in strain at break with the addition of 10 wt% of C10A to chitosan was reported by Oguzlu and Tihminlioglu.[120] The improvement in tensile strength can be described as the formation of an exfoliated/intercalated state and the uniform dispersion of clay in the chitosan matrix or the strong interaction between chitosan and clay.

Lavorgna *et al.*[131] studied the mechanical properties in tensile mode of chitosan/MMT nanocomposite films in the presence of glycerol as a plasticizer using a nanoindentation technique. In the case of films containing glycerol, the tensile strength is considerably higher than that of neat chitosan with only glycerol. The presence of glycerol changes the hydrogen-bonding network within the material and allows both a better interaction between the nanofiller and matrix and a higher extent of chitosan intercalation in Na-MMT clay. An increase in storage modulus and glass transition temperature was also observed for the nanocomposite films, from DMA analysis.

2.5.2.2 Thermal Properties

In general, it has been reported that the polymer/clay nanocomposites are thermally more stable than neat polymers. The effect of clay layers has usually been attributed to superior insulation and a mass transport barrier against the volatile compounds generated during the decomposition of polymer chains under thermal conditions. Clay minerals are inorganic materials and are largely stable in the temperature ranges when organic polymers are degraded into volatile compounds.[40,138,139] Compositional analysis is often made using thermogravimetric analysis (TGA), which can separate fillers, polymer resin, and other additives. TGA can also give an indication of thermal stability and the effects of additives. TGA measures the amount and rate (velocity) of change in the mass of a sample as a function of temperature or time in a controlled atmosphere. Differential scanning calorimetry (DSC) is another widely used technique for examining polymers to check their composition, melting point, and polymer degradation. In this method, the difference in the amount of heat required to increase the temperature of a sample and reference is measured as a function of temperature. Thermal properties of chitosan/MMT nanocomposites have been analyzed and compared with that of neat chitosan under various oxidative (air) or non-oxidative (inert gases) environments.

Wang *et al.*[140] reported a systematic improvement in the thermal stability of a chitosan matrix by the incorporation of nanodispersed MMT clay, studied by TGA and differential thermogravimetry (DTG) under both nitrogen and air flows. The degradation patterns for neat chitosan or derivatives of chitosan and their nanocomposites with pristine MMT were different, indicating two different mechanisms for the composite degradation (Figure 2.10). Under a nitrogen atmosphere there are two steps of degradation. The first range (50–200 °C) is associated with the loss of water by about 5–8 wt%, whereas the
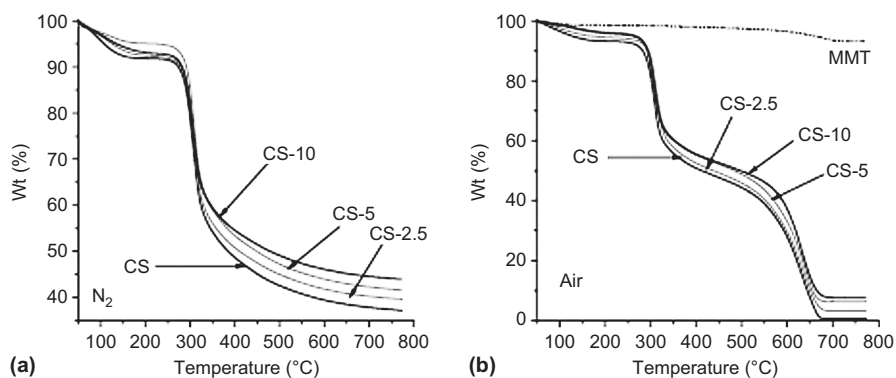

Figure 2.10   TGA curves of MMT, chitosan (CS), and various nanocomposites (wt% MMT): (a) CS, CS-2.5, CS-5, and CS-10 in a nitrogen flow; (b) MMT, CS, CS-2.5, CS-5, and CS-10 in an air flow.
(Reproduced with permission from Wang *et al.*[140])

second range (200–450 °C) corresponds to the degradation and deacetylation of chitosan and leaves about 50 wt% solid residue.

In the air flow, there exists another degradation step (450–700 °C) with a maximum decomposition rate around 600 °C, which may be assigned to the oxidative degradation of the carbonaceous residue formed during the former step. The chitosan/MMT composites containing residual acetic acid showed lower thermal stability than the composites free from acetic acid.

At 50% weight loss, the decomposition temperature of CS/MMT nanocomposites with 2.5 to 10 wt% MMT are 25–100 °C higher than that of pure CS. The clay acts as a heat barrier as well as assisting in the formation of char after thermal decomposition. The nano-dispersed lamellae of clay in the polymer matrix will result qualitatively in a spatially more uniform and thicker char during decomposition. The nano-dispersed clay enhances the formation of char on the surface of the polymer matrix and, as a consequence, reduces the rate of decomposition.

In another study, Wang et al.[123] compared the thermal stability of two different chitosan derivatives (*N,O*-carboxymethyl chitosan and *N,N,N*-trimethyl chitosan chloride) and their MMT-containing nanocomposites. For the carboxymethyl chitosan/MMT system, with respect to neat chitosan/MMT the thermal stability was higher. However, fast degradation in the early thermal stage of the nanocomposites was observed in the case of the trimethyl chitosan/MMT nanocomposites.

The thermal properties of chitosan/MMT nanocomposites containing CNa and C30B were analyzed by DSC and TGA by Xu et al.[46] DSC plots of chitosan and the corresponding CNa-containing nanocomposites are presented in Figure 2.11. Two endothermic peaks, one at 102 °C (attributed to the solvent evaporation) and another one in the range of 168–196 °C, showed that the crystallization of the chitosan was not inhibited by the nanoclays. Pure chitosan film had a melting temperature (T_m) of 193.6 °C and a melting enthalpy (ΔH_m) of 6.05 J g^{-1}.

Addition of 1 and 3 wt% of CNa increased the T_m to 196 °C and the ΔH_m to 11 J g^{-1}, respectively. However, the T_m of the composite film decreased to 194.5 °C when the amount of CNa was increased to 5 wt%. On the other hand, both T_m and ΔH_m decreased with the addition of C30B, suggesting that the degree of crystallinity of chitosan was reduced. The well dispersed C30B acted as a physical barrier to hinder the growth of crystals and their perfect ordering.[141] An increase in thermal stability of chitosan/MMT films was also observed when CNa was used as a nanofiller. This was reflected by the fact that the onset temperatures for thermal degradation increased by 12 and 7 °C with the incorporation of 1 and 3 wt% CNa, respectively, into the chitosan matrix, owing to the formation of nanoscale composites. On the other hand, the onset degradation temperature of chitosan films did not increase significantly with the addition of C30B because of tactoid formation. Günister and co-workers[142] and Han et al.[119] also reported higher thermal stability for chitosan/pristine MMT composites. Because inorganic species have good thermal stabilities, it is generally believed that the introduction of inorganic components into organic
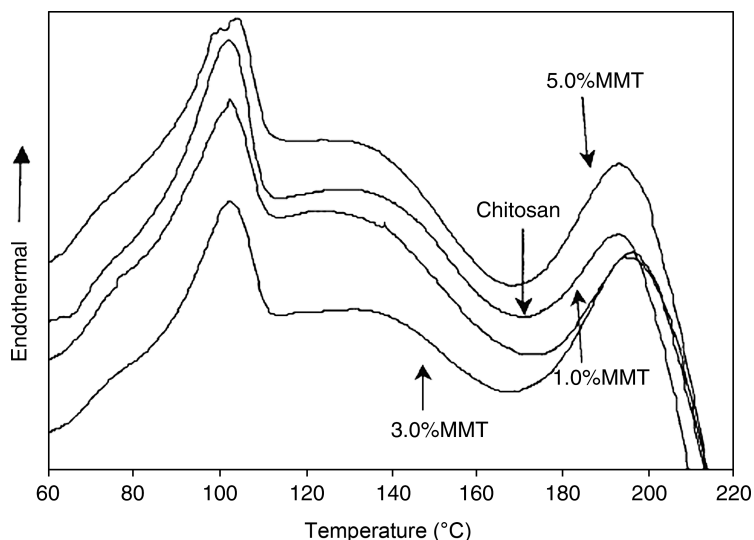
Figure 2.11 DSC thermographs of chitosan and its MMT (CNa) nanocomposites with different MMT contents.
(Reproduced with permission from Xu *et al.*[46])

materials can improve their thermal stability. This increase in the thermal stability can be attributed to the high thermal stability of clay and to the interaction between the clay particles and the chitosan.

Depan *et al.*[143] investigated the effect of Na-MMT on the thermal properties of chitosan-*g*-lactic acid films prepared by solvent casting. The thermal decomposition profile showed that the maximum decomposition temperature was for nanocomposites with a clay loading of 5 and 10%. With further increase in clay content, the thermal stability decreased. The addition of clay enhanced the thermal properties by acting as a superior insulator and mass transport barrier to the volatile products generated during decomposition. Enhancement in the thermal stability of hybrid nanocomposites of poly(butyl acrylate) and chitosan with the introduction of TRIAB-modified MMT was reported by Yu and co-workers.[115] Because of its inherent high thermal and barrier properties the organoclay can prevent the heat from transmitting quickly and can limit the continuous decomposition of the nanocomposites.

2.5.2.3 Barrier Properties

The barrier properties of chitosan can be significantly altered by inclusion of inorganic platelets with sufficient aspect ratio to alter the diffusion path of penetrant molecules. Clay sheets are naturally impermeable. Clays increase the barrier properties of polymers by creating a maze or complex path that retards the diffusion of gas molecules through the polymer matrix. The degree of

enhancement in the barrier properties depends on the degree of tortuosity
created by the clay layers in the diffusion path of molecules through the
polymer film, which in turn depends on the aspect ratio of the clay. Increasing
the side length of the clay sheet, as well as increasing the exfoliation or degree of
dispersion, results in barrier enhancement in the polymer matrix. Many studies
have reported the barrier properties of chitosan/MMT nanocomposites against
the diffusion of gases and water vapour.[141,144,145]

Assuming silicate layers as crystalline lamellae in the matrix in a semi-crys-
talline polymer based on Klute's theory,[146] the permeability P of composites is
$P = P_0(1 - \Phi_s)\zeta(\Phi_s)$, where P_0, Φ_s, and ζ are the permeability of the matrix in
the composite, the clay layers volume fraction, and a function for the reduction
of the permeability due to the clay layers in the polymer matrix, respectively.
Thus, the relative permeability for composites can be obtained as the following
equation: $R_p = (1 - \Phi_s)\zeta(\Phi_s)$. Nielsen[147] formulated a detour model for
the rectangular filler particles, with length and width l and thickness d.[148] For
the clay platelets dispersed parallel in a polymer matrix, the tortuosity factor
can be formulated as: $\tau = 1 + (l/2d)\phi_{clay}$, where ϕ_{clay} is the volume fraction of
the dispersed clay particles.

A typical test method provides the determination of gas transmission rate
(GTR), the permeance of the film to gas (P), the permeation coefficient of the
film to its thickness, and permeability coefficient in the case of homogeneous
materials at given temperature and relative humidity (%RH) level.

Rhim *et al.*[116] studied the water vapour permeability (WVP) for chitosan-
based nanocomposite films containing different types of nanofillers and the
results are summarized in Table 2.4. The WVP value of the chitosan film was
$(1.31 \pm 0.07) \times 10^{-12}$ kg m^{-1} s^{-1} Pa^{-1}. The WVP of the nanocomposite films
decreased significantly ($P < 0.05$) by 25–30%, depending on the nanoparticles
used. Among the nanocomposite films tested, the chitosan/C30B film had the
lowest WVP, showing improvement in barrier properties which may be due to
the development of a complex composite structure of chitosan with organoclay
nanoparticles. However, this particular nanocomposite showed the highest
hydrophilicity (lowest contact angle), against expectations (usually, the more

Table 2.4 Water vapour barrier and water resistance properties of chitosan-
based nanocomposite films.[a]

Film type	MC (wt%)	WVP (10^{-12} kg m^{-1} s^{-1} Pa^{-1})	RH (%)	CA (°)	WS (%)
Neat chitosan	27.1 ± 0.8a	1.31 ± 0.07	76.2 ± 1.4	45.6 ± 0.2	13.6 ± 1.1
Na-MMT	26.4 ± 0.4a	0.98 ± 0.15	78.8 ± 0.6	47.4 ± 0.2	12.5 ± 0.8
Cloisite 30B	24.3 ± 0.2b	0.92 ± 0.03	78.2 ± 0.2	43.4 ± 1.3	13.2 ± 1.0
Nano-silver	24.5 ± 0.0b	0.95 ± 0.12	78.1 ± 0.2	48.5 ± 1.1	14.1 ± 0.8
Ag-ion	22.3 ± 0.3c	0.96 ± 0.05	77.3 ± 0.4	50.4 ± 1.0	15.4 ± 0.6

[a]MC, moisture content; WVP, water vapour permeability; RH, actual relative humidity value
underneath the film covering the WVP measuring cup; CA, contact angle of water drop; WS, water
solubility.

hydrophilic a material is, the lower the contact angle value it has; the orga-
noclay by nature is hydrophobic).

Oguzlu and Tihminlioglu[120] investigated the water vapour and oxygen per-
meabilities of pure chitosan and chitosan/C10A nanocomposite films at a
constant temperature (23 °C) and relative humidity (0% RH) conditions with
5–10 cm^3 min^{-1} gas flow. The WVP of the chitosan nanocomposite films was
significantly reduced even in the 2 wt% clay-containing chitosan film. More-
over, the WVP decreased as the clay content increased in the polymer matrix.
The WVP of pure chitosan was found to be 3.4 g mm m^{-2} d^{-1} mmHg^{-1},
whereas for the composite films the value decreased to as low as 2.4 g mm
m^{-2} d^{-1} mmHg^{-1}, *i.e.* by 20–27% depending on the clay loading.

For all clay loadings the nanocomposite films were better oxygen barriers
than the pure chitosan film, exhibiting 83–92% reduction in oxygen perme-
ability with the addition of 2–10 wt% clay in the chitosan. The decrease in
permeabilities of the nanocomposite films is believed to be due to the presence
of ordered dispersed particle layers with large aspect ratios in the polymer
matrix. As a consequence of the decrease in permeability, the barrier properties
of chitosan for use in food packaging, protective coating, and other applica-
tions can be improved with the addition of clay to the polymer matrix.

The effect of shear rate on the barrier properties during homogenization of
Na-MMT into the chitosan matrix was reported by Hong *et al.*[149] Oxygen and
water vapour permeabilities decreased dramatically as the amount of Na-MMT
increased up to 5 wt%, and it did not change significantly with only a little
increase above 5 wt%. The lowest values for oxygen and water vapour per-
meabilties were 4.2×10^{-19} kg m^{-1} s^{-1} Pa^{-1} and 1240 g m^{-1} s^{-1} Pa^{-1}, respec-
tively, at a shear rate of 16 000 rpm. Therefore, homogenization at an optimal
shear rate of 16 000 rpm is an effective method for dispersing Na-MMT in a
chitosan polymer matrix to improve the barrier properties.

2.5.2.4. Water Swelling Properties

The water absorption property of chitosan-based nanocomposites is very
important, depending on the application for which they are envisaged. For
packaging applications, materials need good water resistance to maintain their
physical strength. On the other hand, for superabsorbent materials for drug
delivery and waste water treatment, a higher water or pH swelling capacity is
required. So the water swelling property becomes an important characteristic of
chitosan/MMT nanocomposites. In a typical procedure, a specific amount of
chitosan/MMT composite was immersed in an excess of distilled water at room
temperature for 8 h to reach the swelling equilibrium. Swollen samples were
then separated from unabsorbed water either by filtering or using blotting
paper. Water absorbency of the material was then calculated gravimetrically.

Yu *et al.*[115] also carried out a similar study on chitosan-*g*-poly(butyl acrylate)
hybrid nanocomposites containing TRIAB-modified MMT. The results
showed a decreasing trend of water absorption percentage with the increase of
organoclay concentration (Table 2.5). This could be attributed to the large

Table 2.5   Water absorption of chitosan-*g*-poly(butyl acrylate)/MMT nano-
                composites as a function of MMT content.

MMT conc. (wt%)	0	3	5	7
Water absorption (%) at 24 h	133.2	82.2	80.5	75.6

numbers of cross-linking points created by organo-MMT in the polymer matrix, which prevents water absorption. However, Zhang *et al.*[125] reported higher water absorption capacity for chitosan-*g*-poly(acrylic acid)/MMT nanocomposites prepared by *in situ* intercalative polymerization when compared to the absorption property of similar nanocomposites prepared by a two-step method. The MMT during the *in situ* polymerization could form a loose and porous surface, with improved water absorbency of the chitosan-*g*-poly-(acrylic acid) superabsorbent.

Depan and co-workers[48] studied the water swelling properties of chitosan-*g*-lactic acid/MMT nanocomposite scaffolds. The swelling behaviour and water retention properties of the nanocomposites were found to be significantly higher than pure chitosan film. The MMT acts as a physical barrier and prevents moisture from exuding out of the films. In tissue engineering applications, during the course of cell proliferation the retained hydrophilicity of the scaffold would enhance cell attachment and proliferation on its surface.

2.5.2.5   Other Properties

The higher adsorption property of chitosan/MMT composites when compared to pure chitosan for Congo red dye was reported by Wang and Wang.[126] The dye adsorption process was also found to be dependent on the molar ratio of chitosan to MMT (adsorption increased from 1:10 to 1:1) and the initial pH value of the dye solution and temperature. In another study,[127] they compared the adsorption capacity of CTAB-modified MMT with that of chitosan/organo-MMT nanocomposites. The nanocomposite exhibited higher adsorption capacities for Congo red when the molar ratio of chitosan to organo-MMT was less than 10:1. The same group reported the adsorption characteristics of methylene blue on chitosan-*g*-poly(lactic acid)/MMT hybrid composites.[150] According to the results, composites containing 2 wt% MMT clay showed the highest adsorption property when compared to the other samples. The interaction of the OH groups of MMT during graft polymerization and MMT exfoliation in the polymer matrix helps to create a loose and porous structure with improved adsorption capacity. At higher clay loadings the interaction among MMT, chitosan, and monomer becomes intensive, leading to more chemical and physical cross-linkages whereby the elasticity of the polymer chains decreases, which decreases the adsorption capacity of the nanocomposite. Improved adsorption properties of chitosan/MMT nanocomposites for tannic acid were also reported by An and Dultz.[151]

Rhim and co-workers[152] investigated the antimicrobial properties of chitosan films containing CNa and C30B. The analyses showed that the

C30B-incorporated film showed significantly higher antimicrobial activity against food pathogenic bacteria (*S. aureus* and *L. monocytogenes*) than Na-MMT-incorporated film, even though the basic structure of MMT is the same for both. This may be attributed to the antimicrobial activity of the quaternary ammonium group in the silicate layer of the C30B-incorporated film. The effectiveness of such groups bearing alkyl substituents is more effective in disrupting bacterial cell membranes and causing cell lyses. Han *et al.*[119] also reported increased antibacterial properties for chitosan/MMT nanocomposites against pure chitosan and MMT. Shameli *et al.*[132] recently studied the antimicrobial property of chitosan/MMT composites containing Ag nanoparticles. According to the results, introduction of Ag nanoparticles improves the antibacterial property of chitosan/MMT nanocomposites. Ag nanoparticles, because of their size and greater surface area, can easily reach the nuclear content of bacteria.

Günister *et al.*[142] studied the rheological properties of chitosan/MMT colloidal dispersions. The rheological parameters such as viscosity, yield value, and apparent and plastic viscosity were reduced by the addition of MMT to the chitosan dispersions, which indicated that the clay particles caused the decrease in the resistance of the polymer against the flow. The negatively charged clay particles interacted with the positively charged polymer electrostatically by attaching them to its surface, allowing the flow to proceed more easily.

2.6 Applications of Chitosan/MMT Nanocomposites

Chitosan is one of the most abundant naturally occurring macromolecules and the new class of composites based on chitosan and MMT clay dispersed at a nanometric level can result in low cost, highly competitive, and environmentally friendly materials for a variety of applications. The incorporation of MMT nanoclay into the chitosan matrix is suitable for the improvement of physical, barrier, and antimicrobial properties of the neat chitosan. These improved properties brought by the nanofiller could present a wide range of possibilities, such as packaging, electrochemical devices, super adsorbent, or biomedical applications.

One of the widely researched applications of chitosan/MMT nanocomposites is as biodegradable active packaging materials. Incorporation of nanostructured MMT (either pristine or organically modified) into the chitosan matrix results in improved mechanical properties, water vapour and oxygen barrier properties, and thermal stability of the resulting nanocomposites without sacrificing biodegradability. Such property improvements are generally attained at low nanoclay content (less than 5 wt%) compared to that of conventional fillers (in the range of 10–50 wt%). For these reasons, nanocomposites are far lighter in weight than conventional composite materials, making them competitive with other materials for packaging.[40,104] Moreover, the application of these materials can be expanded by adding multiple functionalities like antimicrobial and antioxidation properties. Different types of nanoparticles can be used as additives in this case.

Chitosan/MMT nanocomposites have gained great attention as effective biosorbents due to their low cost and the high content of amino and hydroxyl functional groups, which show significant adsorption potential for the removal of various aquatic pollutants. The improved adsorption of tannic acid on chitosan beads made of a hybrid of chitosan flake and clay was reported by Chang and Juang.[50] Similar results were obtained on freeze-dried chitosan/MMT composites by An and co-workers.[151] Wang *et al.*[126,127,150] successfully prepared chitosan/MMT nanocomposites and hybrid composites (with pristine and organically modified MMT) and used them efficiently for the removal of organic dyes such as Congo red and methylene blue from aqueous effluents.

Another interesting application of chitosan/MMT nanocomposites is as electrochemical sensors. The intercalation of the cationic biopolymer chitosan in MMT provides a robust nanocomposite with anionic exchange properties.[113] These materials have been successfully used in the development of bulk-modified electrodes applied to the potentiometric determination of several anions with a high selectivity towards monovalent anions, such as NO_3^-, CH_3COO^-, and Cl^-. Although the resulting sensors are used in the determination of several anions, the remarkable selectivity towards monovalent anions may be attributed to the special conformation of the biopolymer in the clay interlayer space. The high affinity between the chitosan and the MMT substrate is the basis of the high stability of the intercalated biopolymer against desorption or degradation, and, consequently, of the long-term stability of the developed sensors.[114]

The potential use of novel hybrid composites of chitosan/MMT in controlled drug delivery and tissue engineering applications is also widely investigated. In such drug delivery systems, the drug is stored in the interlayer region of the lamellar host, and the drug is released as a consequence of diffusion and/or a de-intercalation process by controlling the interaction between the host and the drug. In chitosan/MMT nano-hydrogels, the incorporation of negatively charged delaminated MMT electrostatically interacts with the positively charged NH_3^+ group of chitosan to generate a strong cross-linked structure, which greatly affects the macroscopic property of the nano-hydrogel and the drug diffusion through the bulk entity.[48,153]

Liu *et al.*[153] prepared nano-hydrogels composed of chitosan and MMT for the controlled release of vitamin B_{12} under electrostimulation. Under an applied voltage, the drug release behaviour was strongly influenced by the concentration of MMT, which affected the cross-linking density of the nano-hydrogels. The electro-responsiveness of the nano-hydrogel with higher MMT concentrations was reduced, but its anti-fatigue behaviour was considerably improved. The nano-hydrogel with 2 wt% MMT achieved a mechanically reliable and practically desirable pulsatile release profile and excellent anti-fatigue behaviour, compared with that of pure chitosan. Depan *et al.*[48] reported the use of a chitosan-g-lactic acid/MMT porous scaffold for the controlled release of an anticancer drug. According to the results, clay reinforcement to the chitosan matrix contributes significantly to the mechanical, swelling, and controlled drug release properties of the resultant nanocomposite materials.

Controlled release of ofloxacin using chitosan/MMT nanocomposite hydrogels
was investigated by Hua and co-workers.[154] Compared to pure chitosan beads,
the incorporation of MMT enhanced the drug entrapment, improved the
swelling behaviour, and reduced the drug release. The observations suggested
that the electrostatic interaction between chitosan and MMT enhanced the
stability of the beads and showed good potential for the use as drug carriers for
sustained release. Recently, Nanda *et al.*[122] reported the improved drug
releasing properties of a blend containing chitosan, poly(lactic acid), and C30B
for the anticancer drug paclitaxel.

2.7   Current Research Status and Future Scope

This chapter summarizes the preparation, characterization, properties, and
applications of chitosan/MMT nanocomposites. Solvent casting and solution
mixing have been shown as feasible methods of preparation for various chit-
osan/MMT nanocomposites. Chitosans with varying degrees of deacetylation
and different types of MMTs (Na-MMT and organically modified MMT with
different surfactants) have been used for the preparation of nanocomposites.
Hybrid polymer matrices containing chitosan and other biodegradable poly-
mers, such as poly(lactic acid), poly(butyl acrylate), *etc.*, are suggested to be
advantageous in improving the nanocomposite properties. It has been clearly
demonstrated that different parameters, such as MMT dispersion (tactoid,
intercalated, or exfoliated), chitosan/MMT affinity, and clay content, can affect
the structure and the bionanocomposite properties. It has to be noted that the
higher reinforcing effect is generally limited to small clay amounts (<5 wt%)
and is reached for exfoliated states. In the case of good exfoliation and dis-
persion of MMT clays, the mechanical properties, thermal stability, bio-
degradability, and barrier properties were generally improved. These new
materials open up a range of applications in which chitosan can be moulded
into a variety of structures such as hydrogels, films, powders, or even colloids.

The development of novel polymeric materials based on chitosan presents a
very interesting and promising approach in the context of concerns about
environmental waste problems. On the basis of the current literature on chit-
osan/MMT nanocomposites, exceptionally strong future prospects can be
predicted for these materials, which will broaden the scope of applications. In
spite of improvements in mechanical, thermal, and barrier properties that have
been reported, these are not sufficient for petroleum-based plastics to be
replaced. The development of optimum formulations and processing methods
to obtain the desired properties to meet a spectrum of applications, as well as
cost reduction of the bionanocomposites, still needs serious attention. The
possibility of chitosan modification to make it more compatible with MMT
nanostructures, the development of melt intercalation techniques, blending
chitosan with one or more natural biopolymers or other biodegradable poly-
mers, changing the chemistry of MMT nanoclays, *etc.*, are expected to make an
impact in chitosan nanocomposite research in the future.

Acknowledgments

References

1. D. R. Paul and L. M. Robeson, *Polymer*, 2008, **49**, 3167–3204.
2. M. Kawasumi, *J. Polym. Sci., Part A: Polym. Chem.*, 2004, **42**, 819–824.
3. J. J. Kester and O. R. Fennema, *Food Technol.*, 1986, **40**, 47–59.
4. C. S. K. Reddy, R. Ghai, Rashmi and V. C. Kalia, *Bioresour. Technol.*, 2003, **87**, 137–146.
5. R. G. Sinclair, *J. Macromol. Sci., Pure Appl. Chem.*, 1996, **33**, 585–597.
6. R. A. Gross and B. Kalra, *Science*, 2002, **297**, 803–807.
7. H. Tsuji and Y. Ikada, *J. Appl. Polym. Sci.*, 1998, **67**, 405–415.
8. S. Guilbert, B. Cuq and N. Gontard, *Food Addit. Contam.*, 1997, **14**, 741–751.
9. S. Guilbert, N. Gontard and L. G. M. Gorris, *LWT Food Sci. Technol.*, 1996, **29**, 10–17.
10. A. Redl, M. H. Morel, J. Bonicel, B. Vergnes and S. Guilbert, *Cereal Chem.*, 1999, **76**, 361–370.
11. L. Avérous and N. Boquillon, *Carbohydr. Polym.*, 2004, **56**, 111–122.
12. M. Neus Angles and A. Dufresne, *Macromolecules*, 2000, **33**, 8344–8353.
13. J. J. G. van Soest, K. Benes, D. De Wit and J. F. G. Vliegenthart, *Polymer*, 1996, **37**, 3543–3552.
14. K. J. Edgar, C. M. Buchanan, J. S. Debenham, P. A. Rundquist, B. D. Seiler, M. C. Shelton and D. Tindall, *Prog. Polym. Sci.*, 2001, **26**, 1605–1688.
15. S. C. M. Fernandes, C. S. R. Freire, A. J. D. Silvestre, C. Pascoal Neto, A. Gandini, L. A. Berglund and L. Salmén, *Carbohydr. Polym.*, 2010, **81**, 394–401.
16. R. Jayakumar, N. Selvamurugan, S. V. Nair, S. Tokura and H. Tamura, *Int. J. Biol. Macromol.*, 2008, **43**, 221–225.
17. F. Chivrac, E. Pollet and L. Avérous, *Mater. Sci. Eng. R*, 2009, **67**, 1–17.
18. Q. Li, E. T. Dunn, E. W. Grandmaison and M. F. A. Goosen, *J. Bioact. Compat. Polym.*, 1992, **7**, 370–397.
19. C. Peniche, W. Argüelles-Monal and F. M. Goycoolea, in *Monomers, Polymers and Composites from Renewable Resources*, ed. M. Belgacem and A. Gandini, Elsevier, Amsterdam, 2008, pp. 517–542.
20. H. Nagahama, N. Nwe, R. Jayakumar, S. Koiwa, T. Furuike and H. Tamura, *Carbohydr. Polym.*, 2008, **73**, 295–302.
21. K. Madhumathi, P. T. Sudheesh Kumar, K. C. Kavya, T. Furuike, H. Tamura, S. V. Nair and R. Jayakumar, *Int. J. Biol. Macromol.*, 2009, **45**, 289–292.

22. R. Jayakumar, M. Prabaharan, R. L. Reis and J. F. Mano, *Carbohydr. Polym.*, 2005, **62**, 142–158.
23. M. Peter, N. Ganesh, N. Selvamurugan, S. V. Nair, T. Furuike, H. Tamura and R. Jayakumar, *Carbohydr. Polym.*, 2010, **80**, 687–694.
24. K. Muramatsu, S. Masuda, Y. Yoshihara and A. Fujisawa, *Polym. Degrad. Stab.*, 2003, **81**, 327–332.
25. X. Lu, Q. Zhang, L. Zhang and J. Li, *Electrochem. Commun.*, 2006, **8**, 874–878.
26. J. M. Oliveira, M. T. Rodrigues, S. S. Silva, P. B. Malafaya, M. E. Gomes, C. A. Viegas, I. R. Dias, J. T. Azevedo, J. F. Mano and R. L. Reis, *Biomaterials*, 2006, **27**, 6123–6137.
27. X. D. Liu, N. Nishi, S. Tokura and N. Sakairi, *Carbohydr. Polym.*, 2001, **44**, 233–238.
28. K. Kurita, *Mar. Biotechnol.*, 2006, **8**, 203–226.
29. T. Yui, K. Imada, K. Okuyama, Y. Obata, K. Suzuki and K. Ogawa, *Macromolecules*, 1994, **27**, 7601–7605.
30. D. Schmidt, D. Shah and E. P. Giannelis, *Curr. Opin. Solid State Mater. Sci.*, 2002, **6**, 205–212.
31. J. M. Krochta and C. De Mulder-Johnston, *Food Technol.*, 1997, **51**, 61–74.
32. M. R. de Moura, F. A. Aouada, R. J. Avena-Bustillos, T. H. McHugh, J. M. Krochta and L. H. C. Mattoso, *J. Food Eng.*, 2009, **92**, 448–453.
33. T. H. McHugh and J. M. Krochta, *J. Am. Oil Chem. Soc.*, 1994, **71**, 307–312.
34. I. J. Roh and I. C. Kwon, *J. Biomater. Sci., Polym. Ed.*, 2002, **13**, 769–782.
35. M. I. G. Siso, E. Lang, B. Carrenő-Gómez, M. Becerra, F. Otero Espinar and J. Blanco Méndez, *Process Biochem.*, 1997, **32**, 211–216.
36. N. L. Akers, C. M. Moore and S. D. Minteer, *Electrochim. Acta*, 2005, **50**, 2521–2525.
37. A. K. Mohanty, M. Misra and L. T. Drzal, *J. Polym. Environ.*, 2002, **10**, 19–26.
38. M. Wollerdorfer and H. Bader, *Ind. Crops Prod.*, 1998, **8**, 105–112.
39. M. Alexandre and P. Dubois, *Mater. Sci. Eng. R*, 2000, **28**, 1–63.
40. S. Sinha Ray and M. Okamoto, *Prog. Polym. Sci.*, 2003, **28**, 1539–1641.
41. O. E. Gain, E. Espuche, E. Pollet, M. Alexandre and P. Dubois, *J. Polym. Sci., Part B: Polym. Phys.*, 2005, **43**, 205–214.
42. G. Gorrasi, M. Tortora, V. Vittoria, E. Pollet, M. Alexandre and P. Dubois, *J. Polym. Sci., Part B: Polym. Phys.*, 2004, **42**, 1466–1475.
43. E. Picard, A. Vermogen, J. F. Gérard and E. Espuche, *J. Membr. Sci.*, 2007, **292**, 133–144.
44. X. Y. Wang, B. Liu, R. C. Sun and J. Wu, *Huanan Ligong Daxue Xuebao/ J. South China Univ. Technol. (Nat. Sci.)*, 2010, **38**, 96–101.
45. M. Darder, M. L. Blanco, P. Aranda, A. J. Aznar, J. Bravo and E. Ruiz-Hitzky, *Chem. Mater.*, 2006, **16**, 1602–1610.
46. Y. Xu, X. Ren and M. A. Hanna, *J. Appl. Polym. Sci.*, 2006, **99**, 1684–1691.

47. H. Hua, H. Yang, W. Wang and A. Wang, *Appl. Clay Sci.*, 2010, **50**, 112–117.
48. D. Depan, A. P. Kumar and R. P. Singh, *Acta Biomater.*, 2009, **5**, 93–100.
49. H. Gecol, E. Ergican and P. Miakatsindila, *J. Colloid Interface Sci.*, 2005, **292**, 344–353.
50. M. Y. Chang and R. S. Juang, *J. Colloid Interface Sci.*, 2004, **278**, 16–25.
51. J. Vartiainen, R. Motion, H. Kulonen, M. Rättö, E. Skyttä and R. Ahvenainen, *J. Appl. Polym. Sci.*, 2004, **94**, 986–993.
52. F. Shahidi, J. K. V. Arachchi and Y. J. Jeon, *Trends Food Sci. Technol.*, 1999, **10**, 37–51.
53. C. Caner and O. Cansiz, *J. Sci. Food Agric.*, 2007, **87**, 227–232.
54. M. Peter, N. S. Binulal, S. Soumya, S. V. Nair, T. Furuike, H. Tamura and R. Jayakumar, *Carbohydr. Polym.*, 2010, **79**, 284–289.
55. W. Xia and J. Chang, *Mater. Lett.*, 2007, **61**, 3251–3253.
56. M. Rai, A. Yadav and A. Gade, *Biotechnol. Adv.*, 2009, **27**, 76–83.
57. K. Madhumathi, P. T. Sudheeshkumar, S. Abhilash, V. Sreeja, H. Tamura, K. Manzoor, S. V. Nair and R. Jayakumar, *J. Mater. Sci.: Mater. Med.*, 2010, **21**, 807–813.
58. Z. K. Wang, Q. L. Hu and L. Cai, *Chin. J. Polym. Sci.*, 2010, **28**, 801–806.
59. A. Wei, X. W. Sun, J. X. Wang, Y. Lei, X. P. Cai, C. M. Li, Z. L. Dong and W. Huang, *Appl. Phys. Lett.*, 2006, **89**, 123902–123904.
60. X. M. Luo, A. Morrin, A. J. Killard and M. R. Smyth, *Electroanalysis*, 2006, **16**, 319–326.
61. Y. L. Liu, W. H. Chen and Y. H. Chang, *Carbohydr. Polym.*, 2009, **76**, 232–238.
62. X. Kang, J. Wang, H. Wu, I. A. Aksay, J. Liu and Y. Lin, *Biosens. Bioelectron.*, 2009, **25**, 901–905.
63. X. Yang, Y. Tu, L. Li, S. Shang and X. M. Tao, *Appl. Mater. Interfaces*, 2010, **2**, 1707–1713.
64. Y. Zhu, H. Cao, L. Tang, X. Yang and C. Li, *Electrochim. Acta*, 2009, **54**, 2823–2827.
65. Z. Zainal, L. K. Hui, M. Z. Hussein, A. H. Abdullah and I. R. Hamadneh, *J. Hazard. Mater.*, 2009, **164**, 138–145.
66. A. Kaushik, P. R. Solanki, A. A. Ansari, G. Sumana, S. Ahmad and B. D. Malhotra, *Sens. Actuators B*, 2009, **138**, 572–580.
67. R. L. Qin, F. Li, W. Jiang and L. Liu, *J. Mater. Sci. Technol.*, 2009, **25**, 69–72.
68. F. Y. Cheng, C. H. Su, Y. S. Yang, C. S. Yeh, C. Y. Tsai, C. L. Wu, M. T. Wu and D. B. Shieh, *Biomaterials*, 2005, **26**, 729–738.
69. Y. C. Chang, S. W. Chang and D. H. Chen, *React. Funct. Polym.*, 2006, **66**, 335–341.
70. A. H. Lu, E. L. Salabas and F. Schüth, *Angew. Chem. Int. Ed.*, 2007, **46**, 1222–1244.
71. A. Travan, C. Pelillo, I. Donati, E. Marsich, M. Benincasa, T. Scarpa, S. Semeraro, G. Turco, R. Gennaro and S. Paoletti, *Biomacromolecules*, 2009, **10**, 1429–1435.

72. Y. Du, X. L. Luo, J. J. Xu and H. Y. Chen, *Bioelectrochemistry*, 2007, **70**, 342–347.

73. H. Huang, Q. Yuan and X. Yang, *Colloids Surf. B*, 2004, **39**, 31–37.

74. S. Adewuyi, K. T. Kareem, A. O. Atayese, S. A. Amolegbe and C. A. Akinremi, *Int. J. Biol. Macromol.*, 2011, **48**, 301–303.

75. D. S. Couto, Z. Hong and J. F. Mano, *Acta Biomater.*, 2009, **5**, 115–123.

76. J. Dilag, H. Kobus and A. V. Ellis, *Forensic Sci. Int.*, 2009, **167**, 97–102.

77. S. Ozarkar, M. Jassal and A. K. Agrawal, *Smart Mater. Struct.*, 2008, **17**, 000.

78. O. Z. Zinger, G. Zhao, Z. Schwartz, J. Simpson, M. Wieland, D. Landolt and B. Boyan, *Biomaterials*, 2005, **26**, 1637–1647.

79. Y. Zhou, H. Yang and H. Y. Chen, *Talanta*, 2008, **76**, 419–423.

80. H. Yang, X. H. Yang, Y. Q. Chen and M. Pan, *Chin. J. Anal. Chem.*, 2009, **37**, 275–278.

81. Z. Zhao, W. Lei, X. Zhang, B. Wang and H. Jiang, *Sensors*, 2010, **10**, 1216–1231.

82. M. Yang, F. Qu, Y. Li, Y. He, G. Shen and R. Yu, *Biosens. Bioelectron.*, 2007, **23**, 414–420.

83. P. Matteini, F. Ratto, F. Rossi, S. Centi, L. Dei and R. Pini, *Adv. Mater.*, 2010, **22**, 4313–4316.

84. D. Depan, A. Pratheep Kumar and R. P. Singh, *J. Biomed. Mater. Res. A*, 2006, **78**, 372–382.

85. H. Y. Zhu, R. Jiang and L. Xiao, *Appl. Clay Sci.*, 2010, **48**, 522–526.

86. E. Günister, D. Pestreli, C. H. Ünlü, O. Atici and N. Güngör, *Carbohydr. Polym.*, 2007, **67**, 358–365.

87. S. K. Choudhari, A. A. Kittur, S. S. Kulkarni and M. Y. Kariduraganavar, *J. Membr. Sci.*, 2007, **302**, 197–206.

88. H. Fan, L. Wang, K. Zhao, N. Li, Z. Shi, Z. Ge and Z. Jin, *Biomacromolecules*, 2010, **11**, 2345–2351.

89. Y. Pan, T. Wu, H. Bao and L. Li, *Carbohydr. Polym.*, 2011, **83**, 1908–1915.

90. H. Hu, X. Wang, J. Wang, F. Liu, M. Zhang and C. Xu, *Appl. Surf. Sci.*, 2011, **257**, 2637–2642.

91. H. Van Olphen, *An Introduction to Clay Colloid Chemistry*, Wiley, New York, 1977.

92. S. Sinha Ray, K. Yamada, M. Okamoto, A. Ogami and K. Ueda, *Chem. Mater.*, 2003, **15**, 1456–1465.

93. R. Krishnamoorti, R. A. Vaia and E. P. Giannelis, *Chem. Mater.*, 1996, **8**, 1728–1734.

94. P. Aranda and E. Ruiz-Hitzky, *Chem. Mater.*, 1992, **4**, 1395–1403.

95. Y. H. Yu, C. Y. Lin, J. M. Yeh and W. H. Lin, *Polymer*, 2003, **44**, 3553–3560.

96. J. C. Dai and J. T. Huang, *Appl. Clay Sci.*, 1999, **15**, 51–65.

97. Y. Ke, J. Lü, X. Yi, J. Zhao and Z. Qi, *J. Appl. Polym. Sci.*, 2000, **78**, 808–815.

98. G. Lagaly, *Appl. Clay Sci.*, 1999, **15**, 1–9.

99. Z. Shen, G. P. Simon and Y. B. Cheng, *Polymer*, 2002, **43**, 4251–4260.

AQ2

100. H. R. Fischer, L. H. Gielgens and T. P. M. Koster, *Acta Polym.*, 1999, **50**, 122–126.
101. P. B. Messersmith and E. P. Giannelis, *J. Polym. Sci., Part A: Polym. Chem*, 1995, **33**, 1047–1057.
102. P. Bordes, E. Pollet and L. Avérous, *Prog. Polym. Sci.*, 2009, **34**, 125–155.
103. R. A. Vaia, G. Prince, P. N. Ruth, H. T. Nguyen and J. Lichtenhan, *Appl. Clay Sci.*, 1999, **15**, 67–92.
104. J. W. Rhim and P. K. W. Ng, *Crit. Rev. Food Sci. Nutr.*, 2007, **47**, 411–433.
105. *Polymer-Clay Nanocomposites*, ed. T. J. Pinnavaia and G. W. Beall, Wiley, New York, 2000.
106. P. C. Lebaron, Z. Wang and T. J. Pinnavaia, *Appl. Clay Sci.*, 1999, **15**, 11–29.
107. S. Sinha Ray and M. Okamoto, *Macromol. Rapid Commun.*, 2003, **24**, 815–840.
108. R. A. A. Muzzarelli, in *Proceedings of the First International Conference on Chitin/Chitosan*, ed. R. A. A. Muzzarelli and E. R. Pariser, MIT, Boston, MA, 1978, pp. 335–354.
109. Q. Xin, A. Wirsén and A. C. Albertsson, *J. Appl. Polym. Sci.*, 1999, **74**, 3193–3202.
110. G. Zhao and S. E. Stevens, *Biomaterials*, 1998, **11**, 27.
111. J. W. Rhim and P. K. W. Ng, *Crit. Rev. Food Sci. Nutr.*, 2011, **47**, 411–433.
112. A. Sorrentino, G. Gorrasi, M. Tortora, V. Vittoria, U. Costantino, F. Marmottini and F. Padella, *Polymer*, 2005, **46**, 1601–1608.
113. M. Darder, M. Colilla and E. Ruiz-Hitzky, *Chem. Mater.*, 2003, **15**, 3774–3780.
114. M. Darder, M. Colilla and E. Ruiz-Hitzky, *Appl. Clay Sci.*, 2005, **28**, 199–208.
115. L. Yu, L. Li, Z. Wei'an and F. Yuée, *Radiat. Phys. Chem.*, 2004, **69**, 467–471.
116. K. F. Lin, C. Y. Hsu, T. S. Huang, W. Y. Chiu, Y. H. Lee and T. H. Young, *J. Appl. Polym. Sci.*, 2005, **98**, 2042–2047.
117. X. Wang, Y. Du and J. Luo, *Nanotechnology*, 2008, **19**, 065707–065713.
118. J. W. Rhim, S. I. Hong, H. M. Park and P. K. W. Ng, *J. Agric. Food Chem.*, 2006, **54**, 5814–5822.
119. L. S. Han, S. H. Lee, K. H. Choi and I. Park, *J. Phys. Chem. Solids*, 2010, **71**, 464–467.
120. H. Oguzlu and F. Tihminlioglu, *Macromol. Symp.*, 2010, **298**, 91–98.
121. S. Sahoo, A. Sasmal, D. Sahoo and P. Nayak, *J. Appl. Polym. Sci.*, 2010, **116**, 3167–3175.
122. R. Nanda, A. Sasmal and P.L. Nayak, *Carbohydr. Polym.*, 2011, **83**, 988–994.
123. S. Wang, L. Chen and Y. Tong, *J. Polym. Sci., Part A: Polym. Chem.*, 2006, **44**, 686–696.
124. S. K. Choudhari and M. Y. Kariduraganavar, *J. Colloid Interface Sci.*, 2009, **338**, 111–120.

125. J. Zhang, L. Wang and A. Wang, *Ind. Eng. Chem. Res.*, 2007, **46**, 2497–2502.
126. L. Wang and A. Wang, *J. Hazard. Mater.*, 2007, **147**, 979–985.
127. L. Wang and A. Q. Wang, *J. Chem. Technol. Biotechnol.*, 2007, **82**, 711–720.
128. W. Tan, Y. H. Zhang, Y. S. Szeto and L. B. Liao, *Key Eng. Mater.*, 2007, **334/335**, 825–828.
129. J. P. Zhang and A. Q. Wang, *Express Polym. Lett.*, 2009, **3**, 302–308.
130. H. B. Yao, Z. H. Tan, H. Y. Fang and S. H. Yu, *Angew. Chem. Int. Ed.*, 2010, **49**, 10127–10131.
131. M. Lavorgna, F. Piscitelli, P. Mangiacapra and G. G. Buonocore, *Carbohydr. Polym.*, 2010, **82**, 291–298.
132. K. Shameli, M. B. Ahmed, W. M. Z. W. Yunus, A. Rustaiyan, N. A. Ibrahim, M. Zargar and Y. Abdollahi, *Int. J. Nanomed.*, 2010, **5**, 875–887.
133. M. B. Ahmad, K. Shameli, M. Darroudi, W. M. Z. Wan Yunus and N. A. Ibrahim, *Am. J. Appl. Sci.*, 2009, **6**, 2030–2035.
134. W. Xie, Z. Gao, W. P. Pan, D. Hunter, A. Singh and R. Vaia, *Chem. Mater.*, 2001, **13**, 2979–2990.
135. C. H. Lee, H. B. Kim, S. T. Lim, H. J. Choi and M. S. Jhon, *J. Mater. Sci.*, 2005, **40**, 3981–3985.
136. L. Yu, L. Li, Z. Wei'an and F. Yuée, *Radiat. Phys. Chem.*, 2004, **69**, 467–471.
137. K. F. Lin, C. Y. Hsu, T. S. Huang, W. Y. Chiu, Y. H. Lee and T. H. Young, *J. Appl. Polym. Sci.*, 2005, **98**, 2042–2047.
138. J. Zhu, A. B. Morgan, F. J. Lamelas and C. A. Wilkie, *Chem. Mater.*, 2001, **13**, 4649–4654.
139. J. W. Gilman, *Appl. Clay Sci.*, 1999, **15**, 31–49.
140. S. F. Wang, L. Shen, Y. J. Tong, L. Chen, I. Y. Phang, P. Q. Lim and T. X. Liu, *Polym. Degrad. Stab.*, 2005, **90**, 123–131.
141. M. Tortora, V. Vittoria, G. Galli, S. Ritrovati and E. Chiellini, *Macromol. Mater. Eng.*, 2002, **287**, 243–249.
142. E. Günister, D. Pestreli, C. H. Ünlü, O. Atici and N. Güngö, *Carbohydr. Polym.*, 2007, **67**, 358–365.
143. D. Depan, B. Kumar and R. P. Singh, *J. Biomed. Mater. Res. B*, 2008, **84**, 164–190.
144. E. P. Giannelis, *Adv. Mater.*, 1996, **8**, 29–35.
145. H. C. Koh, J. S. Park, M. A. Jeong, H. Y. Hwang, Y. T. Hong, S. Y. Ha and S. Y. Nam, *Desalination*, 2008, **233**, 201–209.
146. H. C. Koh, *J. Appl. Polym. Sci.*, 1959, **1**, 340–342.
147. L. E. Nielsen, *J. Macromol. Sci., Chem.*, 1967, **A1**, 929–942.
148. B. Xu, Q. Zheng, Y. Song and Y. Shangguan, *Polymer*, 2006, **47**, 2904–2910.
149. S. I. Hong, J. H. Lee, H. J. Bae, S. Y. Koo, H. S. Lee, J. H. Choi, D. H. Kim, S. H. Park and H. J. Park, *J. Appl. Polym. Sci.*, 2011, **119**, 2742–2749.

150. L. Wang, J. Zhang and A. Wang, *Colloids Surf. A*, 2008, **322**, 47–53.
151. J. H. An and S. Dultz, *Appl. Clay Sci.*, 2007, **36**, 256–264.
152. J. W. Rhim, S. I. Hong, H. M. Park and P. K. W. Ng, *J. Agric. Food Chem.*, 2006, **54**, 5814–5822.
153. K. H. Liu, T. Y. Liu, S. Y. Chen and D. M. Liu, *Acta Biomater.*, 2008, **4**, 1038–1045.
154. S. Hua, H. Yang, W. Wang and A. Wang, *Appl. Clay Sci.*, 2010, **50**, 112–117.